2006

Utilization of the Distributed-Hydrology-Soil-Vegetation-Model (DHSVM) To Quantify Streamflow Changes and Slope Failure Probability Following the Snow-Talon Fire Near Lincoln Montana, USA

Eric Lee Tangedahl
The University of Montana

UTILIZATION OF THE DISTRIBUTED-HYDROLOGY-SOIL-VEGETATION-MODEL (DHSVM) TO QUANTIFY STREAMFLOW CHANGES AND SLOPE FAILURE PROBABILITY FOLLOWING THE SNOW-TALON FIRE NEAR LINCOLN MONTANA, USA.

By

Eric Lee Tangedahl

Bachelor of Science, The University of Montana, 2001

Thesis

presented in partial fulfillment of the requirements

for the degree of

Master of Science in Forestry

The University of Montana

Autumn, 2006

Approved by:

Dr. David A. Strobel, Dean
Graduate School

Dr. Donald Potts, Chair
Forestry

Dr. LLoyd P. Queen
Forestry

Dr. Joel E. Henry
Computer Science

Tangedahl, Eric L. M.S., Autumn 2006 Forestry

Utilization of the Distributed-Hydrology-Soil-Vegetation-Model (DHSVM) to Quantify Streamflow Changes and Slope Failure Probability Following the Snow-Talon Fire near Lincoln Montana, USA.

Committee Chair: Don Potts

Models are commonly used to attempt to simulate complex interactions on the landscape. Many factors such as vegetation, soils, topography, weather and disturbances can influence the hydrology of a watershed. Understanding what is influencing changes in streamflow following fire can be difficult due to lack of data or models running at inappropriate resolution.

In dealing with the large spatial extent of approximately 37,000 acres burned at the Snow-Talon Fire near Lincoln Montana and heterogeneous landscape characteristics it is difficult to know the specific regions where mitigation efforts should be focused or what specific influencing factors may be affecting the watershed hydrology. In this study, the Distributed-Hydrology-Soil-Vegetation-Model (DHSVM) was used to identify regions of higher soil failure probability and estimates of pre and post-disturbance stream flows. Because DHSVM is a physically-based distributed parameter model it allowed for the use of high resolution data that more accurately represented landscape parameters such as soils, vegetation, slope, and fire severity. Weather inputs into the model were represented in three-hour increments from two SNOTEL stations and one RAWS. Using the data at a scale of 30 meter pixels, weather at three hour increments and physically based water flux calculations, a detailed simulation of how water moves through the landscape could be visualized. Areas of high soil failure probability can be identified at a per pixel basis. Specific stream reaches can be assessed for maximum expected stream flows.

Working with high spatial resolution data as inputs for DHSVM allowed for results of failure probabilities to be seen at the 30 meter resolution of the digital elevation model. Steamflow values were modeled at 3 hour intervals simulating the influence of daily weather and the varying mosaics of fire disturbance, vegetation types and soils. The ability of DHSVM to model streamflow during calibration was shown in Nash-Sutcliffe efficiency coefficients values of .29 for Blackfoot near Lincoln gauge and to .81 for the Blackfoot below Alice Creek gauge. Simulated peak streamflow following fire increased 66% from the pre-fire conditions.

Acknowledgments

I would like to thank the members of my graduate committee, Don Potts, LLoyd Queen and Joel Henry, for their help and assistance throughout this project. I would also like to thank the National Center for Landscape Fire Analysis for funding this project as well as providing the resources and a wealth of knowledge to make this project a success. Saxon and Andrew from NTSG provided tremendous systems support. I also received great support from Bo Stuart, Chip Fisher and Sue Farley at the Helena National Forest. I would also like to thank my family for their assistance and support.

Table of Contents

List of Tables

List of Figures

Chapter 1: Introduction

Wildfire drastically changes hydrologic response within a watershed. Reduction of vegetative material reduces evapotranspiration and interception of precipitation causing increased overland flow (Neary et al., 2005b; DeBano et al., 1998). Intense heat of fire can create a hydrophobic layer that impedes the infiltration of water increasing surface runoff (DeBano, 2000; Huffman et al., 2001). Areas of high severity fire have been shown to temporarily reduce infiltration capacity due to hydrophobic or water repellant soil conditions (Robichaud, 2000). With fire reducing organic material less water to be retained by vegetation and organic material or by accelerating water to the stream network via overland flow, higher amounts of both water and eroded soil are delivered to the stream channel. This poses a threat to downstream property, fish populations and increases the potential of stream bank erosion.

Factors influencing post-fire runoff and erosion

Changes to the hydrologic cycle can be brought on by the influence of fire on a landscape. Components in the hydrologic cycle such as interception, infiltration, evaporation, soil moisture storage, and overland flow can be substantially impacted by fire (Neary et al., 2005b). I will focus on several of these soil, vegetation, and water factors of which the specifics are detailed in the Rocky Mountain Research Stations General Technical Report - Wildland Fire in Ecosystems, Effects of Fire on Soil and Water.

Interception is a process by which vegetation prohibits a portion of precipitation from reaching the soil in the form of throughfall. The level of fire severity is a critical

factor influencing interception. Fire severity reflects the immediate or primary effects of the fire that are caused by intensity from the fire front and heat released during complete fuel consumption (Brown and Smith, 2000). Depending on the fire severity at specific locations, the amount of vegetation remaining to cause interception will vary. After fire has removed the vegetation this can cause one of the largest changes in hydrologic response when combined with high intensity summer storms(Neary et al., 2005b) .
Infiltration is the process of water entering soil. Higher severity fire can decrease the ability of water to infiltrate into the soil. Fire can reduce infiltration in the following ways (Neary et al., 2005c):

- Collapsing the soil structure due to the removal of vegetative binding material causing an increase in the bulk density of the soil.
- Consequent reduction in soil porosity.
- Raindrop impact on the bare soil surface causing compaction and loss of soil porosity.
- Kinetic forces of raindrop impact displacing soil particles and sealing surface pores.
- Ash and charcoal residue being washing into pores in the soil.

Hydrophobic soils can often be a result of fire burning existing organic layers most commonly between the temperatures of 176ºC and 204ºC (DeBano et al., 1998) creating a waxy layer that impedes the infiltration of water. While hydrophobic soil conditions an naturally exist in areas such as Southern California chaparral shrublands (Neary et al., 2005c) and microbial mycelium by-products (DeBano et al., 1998), hydrophobicity can be intensified by fire. Sandy and course textured soils have been shown to be more susceptible to hydrophobicity (DeBano et al., 1998).

Evaporation from soil, water and plant surfaces combined with plant transpiration is referred to as evapotranspiration. Plant transpiration rates differ due to rooting characteristics, stomatal response, albedo of leaf surfaces and the length of the growing season(Neary et al., 2005c). Because of the usage of water by plants and evaporation off surfaces, the process of evapotranspiration can largely determine the amount of water reaching the stream network in the form of runoff. Fire reduces the amount of vegetation causing a reduction in plant transpiration. Fire can also cause the reduction in large deep rooted trees and replace them with shallow rooted grasses and forbs allowing for less transpiration and more available water for streamflow (Neary et al., 2005b). Soil water storage is increased due to loss of vegetation and subsequent transpiration which allows more of the water to enter and persist within the soil profile. When the soil reaches its maximum water holding capacity or field capacity further added water will result in overland flow contributing to streamflow. Overland flow also occurs when precipitation or snowmelt exceeds the rate at which water can infiltrate into the soil. The resulting overland flow can be a major contributor to flow in intermittent channels eventually reaching the rest of the stream network. When fire reduces interception and infiltration rates overland flow can be much more dramatic causing large increase in stream and flood flow. Flood peak flows can often increase to 100 times that of pre-fire flows (Neary et al., 2005b).

Factors such as soil type, soil saturation, root cohesion, slope, vegetative surcharge and overland flow have been identified in contributing to mass wasting and slope failure events(Doten and Lettenmaier, 2004). The need for forest managers to identify potential areas of soil instability and erosion is evident in the number of tools and techniques that have been developed to estimate soil movement from hill slopes.

Hydrologic modeling

For land management and hazard mitigation issues following fire, it is common to try and model the resulting hydrologic response and erosion potential. Modeling techniques range from watershed wide water balances and statistical regression models identifying influencing factors to deterministic models which attempt to route water and sediment through the watershed using spatially variable data layers. Models can be used to help determine the size of potential flood based on precipitation return probabilities combined with knowledge of landscape conditions.

The Water Resources Evaluation on Non-Point Silvicultural Sources (WRENSS)(Mulkey, 1980) procedures provides quantitative methods for estimating potential changes in stream flow, surface erosion, soil mass movement, total potential sediment discharge and temperature. The WRENSS handbook chapter on soil mass movement specifically addresses issues dealing with hazard assessment. Hazard assessment is broken down into 3 areas: evaluation of stability using soils, geologic, topographic climatic, and vegetative indicators; limited strength-stress analysis of the unstable sites; and estimate of sediment delivery to streams. The objective of this analysis is to determine the natural stability of the site, the sensitivity to natural and anthropogenic soil mass movements, amount of material released, and the amount of soil mass movement delivered to the streams. (Swanston et al., 1980)

One of the most visible changes following fire is the removal of vegetation. This removal of vegetation allows for precipitation to more readily enter the soil profile. Large amounts of precipitation can saturate the soil or exceed the infiltration rate leading to overland flow. The weight of saturated soil combined with reduced root cohesion can cause slope failure.(Wondzell and King, 2003) These methods are just a few examples of tools and techniques for identifying potential erosion and mass wasting.

With increases in computing power, more specific objectives by forest managers and the ability to obtain higher resolution input data (e.g. soils, vegetation, solar radiation and weather), hydrologic modeling has shifted towards spatially distributed, physically based models.(Wigmosta *et al.*, 2002) An example of a spatially distributed lumped parameter model is the Soil and Water Assessment Tool (Neitsch *et al.*, 2002). SWAT uses specific information about weather, soil properties, topography, vegetation and land management practices to model water movement, sediment movement, crop growth, nutrient cycling, etc. The model allows for the watershed to be partitioned into separate sub-basins to reflect dominate land uses or to represent soils with similar hydrologic properties. SWAT contains a weather generator that can produce weather data for each sub-basin in the watershed. Erosion and sediment yield is modeled for each Hydrologic Response Unit (HRU) utilizing the Modified Universal Soil Loss Equation (MUSLE)(Neitsch et al., 2002). By moving away from a lumped sum approach, hydrologic processes can be modeled at the resolution of available data. Satellite and airborne sensor derived data, such as vegetation, fire severity data and DEMs are commonly available at resolutions of 30 meter pixels or smaller.

Distributed Hydrology Soil Vegetation Model (DHSVM) model overview

Hydrology models can most often be categorized into lumped or distributed models. A lumped model does not take into account spatial variability. Distributed models account for the spatial variability of processes, input, boundary conditions and watershed characteristics (Singh, 1995). The spatial accuracy of the data of course depends on the methods by which it was acquired. Distributed hydrology models tend not to generalize an entire basin or sub-basin but rather try to explain variations by using high resolution data. In determining what model one might utilize it depends on the application and the expected outcome or results. Spatial resolution, lump versus distributed, input parameters and output layers all determine how a hydrology model can be applied and on what applications it can be used.

The Distributed Hydrology Soil Vegetation Model (DHSVM) is a physically based distributed parameter model that runs at the spatial resolution of the DEM and at the time series interval of the available weather data. Data inputs necessary to run the model include time series weather data, basin mask file, DEM, soils, vegetation, meteorology, streams, and roads (Lettenmaier, 2006). Environmental Systems Research Institute (ESRI) GIS software Arc/INFO and Arc Map were utilized to create input files and analyze model output. Text configuration files define specific input parameters relating to the data layers. The elevation data provided by the DEM determines the way calculations are made involving shortwave radiation, precipitation, air temperature, and downslope water movement. For each time step of weather data; energy and water flux calculations take place routing water through each grid cell based on the soil and vegetation parameters assigned to that grid cell(Wigmosta et al., 2002). Unsaturated soil moisture movement is calculated using Darcy's Law. Water can then move from one cell to the next recharging or adding to the soil moisture content. Road and stream networks affect routed water by confining the flow to stream channels or from roads down to culverts where the water either continues in a stream network or is allowed to re-infiltrate. Evapotranspiration is handled by first calculating the potential evaporation in the overstory to represent the maximum rate at which vegetation can remove water from the cell(Wigmosta et al., 2002). Intercepted water by the canopy is removed at the potential rate, while water within the cell is removed using the Penman-Montieth approach. Other components of the model include canopy wind resistance, short and long wave radiation, snow accumulation and melt, atmospheric stability, canopy snow interception and release, unsaturated soil moisture movement, saturated subsurface flow, overland flow, and channel flow(Wigmosta et al., 2002). Figure 1 below is a visual representation of water flow through the model as defined by the water flux calculations in DHSVM. For example, in step 3, overland flow is occurring potentially due to rainfall exceeding infiltration, saturated soil not allowing infiltration or hydrophobic conditions. In step 5, water is entering the stream network via infiltration, then being routed in step 6 through defined steam networks.

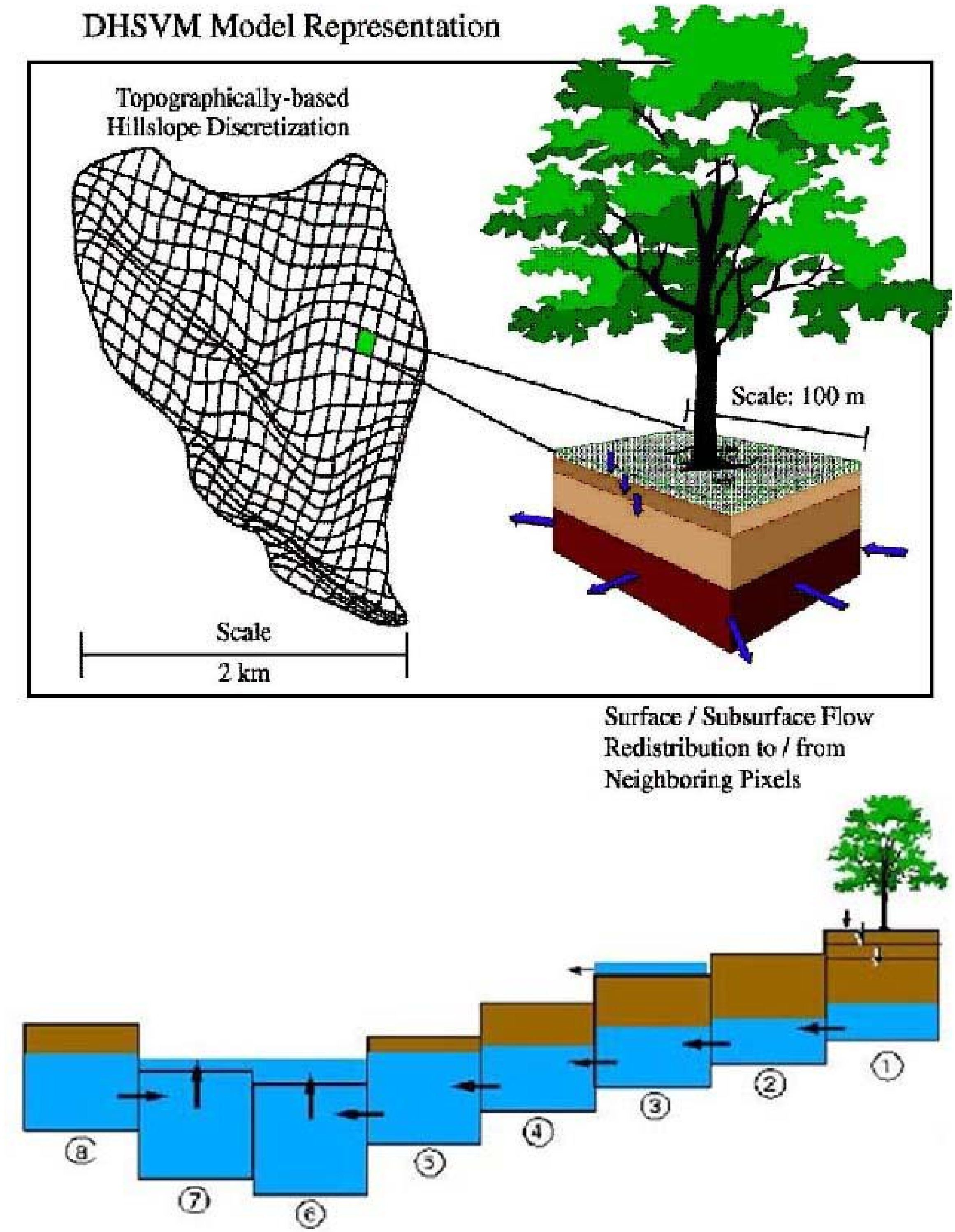

Figure 1 – DHSVM Model Representation (Lanini, 2004)

Rationale for using DHSVM

Selecting the appropriate model is highly dependent on the specific application and the desired results. The number of inputs required in models greatly varies thus changing the usability of the model for certain applications. Models user interfaces can range from graphical user interfaces (GUI) on the web or downloadable application to command line applications that require more knowledge of the necessary inputs of a model. Depending on the resolution of variables you have available to you as well as the resolution of the desired results will change your decision on what model to use. Computing resources will vary depending on the amount of processing power necessary to run certain models. Individual expertise in different fields will be required at times to determine the appropriate inputs of certain variables. It is important prior to choosing a model that these different approaches are taken into consideration. A common outcome of many modeling exercises shows that the output products are too complex or not usable in many management applications.

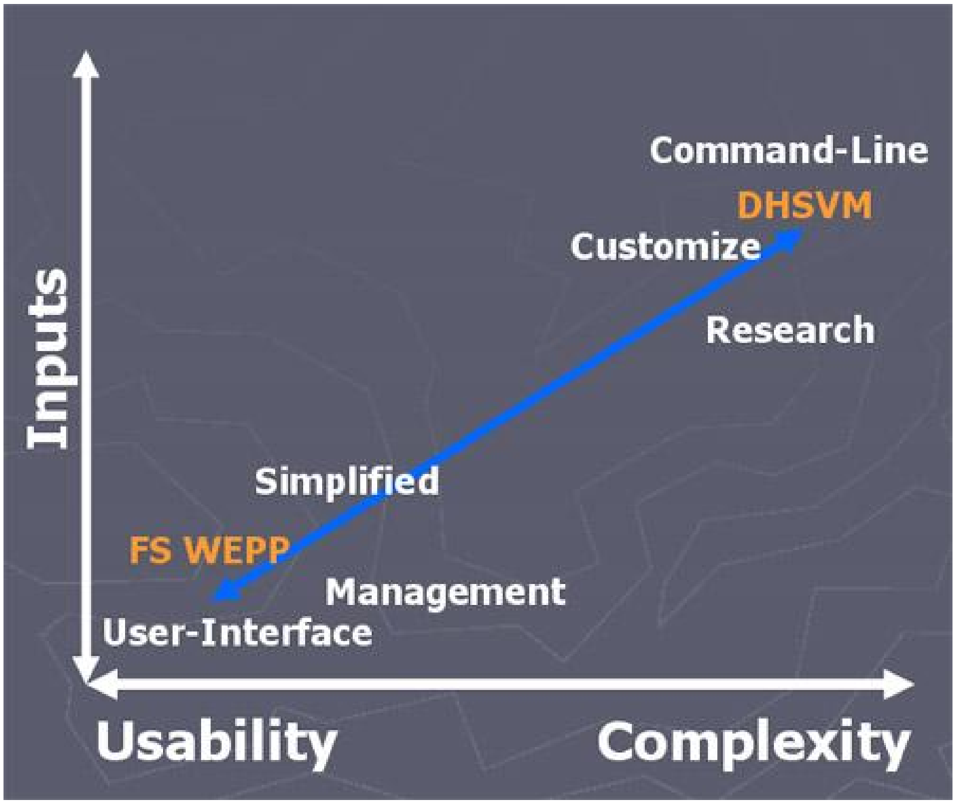

Figure 2 – Differences in model uses

In this thesis I will be using DHSVM to look at pre and post-fire predicted streamflows and failure probabilities following the 2003 Snow-Talon fire near Lincoln, Montana. The objective was to utilize a hydrology model that operates at a scale and timestep of available spatial layers and weather data and thus most accurately represent the site. The decision was made to utilize DHSVM because model calculations are run at the smallest grid-cell (pixel) and a per time-step basis. This allows two items to be looked at: the sensitivity of the data inputs at a single pixel level; the effects of weather at 3-hour increments. Working at the smallest available temporal and spatial scale (provided by the data available) would give the ability to represent specific site locations and the storm characteristics down to the size of a pixel defined by the DEM. Evaluating locations on a per-pixel basis allows more precise location of problematic erosion areas rather than defining an entire sub-basin as problematic. Other models such as SWAT (Neitsch *et al.*, 2002) tend to generalize sub-basin characteristics and not take advantage of currently available data. This may allow for more focused efforts by Burned Area Emergency Rehabilitation (BAER) teams, potentially reducing the costs of treatment in burned areas. Comparisons can then be made between events that occurred on the landscape and how DHSVM modeled those events.

A commonly held assumption for burned areas is that 10.16mm of rain within 15 minutes represents a threshold for erosion events. Others put this threshold around 10mm/hour in 30 minutes (Moody and Martin, 2001), (Robichaud and Brown, 2002) measured intensities in the Bitteroot Valley Montana to range from 3 to 15mm in 10 minutes to 75mm/ hour. This depends on numerous factors but similar intensity thresholds have been used by the National Weather Service when issuing flood warnings in burned drainages (Nickless, 2006). Local conditions tend to affect the threshold therefore there will be variance between locations. (Wondzell and King, 2003) found erosional processes to vary significantly between the Interior Northern Rocky Mountains and Pacific Northwest. Differences in erosion processes were thought to be due to the variability of soils, geology, topography, vegetation and climate between the two regions. While infiltration excess overland flow was a dominate factor in the Interior Region following fire, it had not been documented in the Pacific Northwest. The occurrence of overland flow in the Interior Region was hypothesized to be a result of the frequency of high intensity convective storms during summer months (Wondzell and King, 2003).

DHSVM allows for weather data exceeding certain thresholds to be modeled and the results compared with that of individual cases. Beyond the temporal and spatial scales at which DHSVM calculations are modeled, two recently added components make DHSVM a good choice for modeling post-fire erosion. The Mass Wasting Model-MWM (Doten and Lettenmaier, 2006) and the disturbance component allow the user to choose the specific dates for a disturbance such as fire, and also what time steps to calculate mass wasting probability based on rain events and soil moisture levels. A fire severity grid at the same spatial resolution as the DEM is required for the disturbance component. The MWM runs on the user specified dates and utilizes user-defined soil and vegetation parameters in conjunction with soil moisture values which are calculated for each time step by DHSVM. Because of the additional MWM and disturbance components, DHSVM is designed to specifically handle fire in the watershed (Lanini and Lettenmaier, 2006). More applications of DHSVM on burned watersheds will certainly assist in improving the disturbance component to deal with the many parameters involved in fire. Further explanation of the disturbance and MWM components will follow in Chapter 4.

Chapter 2: Site Description and Data Preparation

The lightning-caused Snow-Talon fire burned just northeast of Lincoln, Montana during the summer of 2003. The fire burned from 8/12/2003 to around 10/15/03, burning approximately 15,259 hectares. Of the total acres burned, 10,724 hectares were mapped as high severity burn. Rehabilitation costs for the fire were $606,400 which included road treatments, hazard tree felling, noxious weed treatment, trail drainage, and monitoring. 348 hectares were deemed a high soil erosion risk (Stuart et al., 2003). With much of the Copper Creek watershed was within the perimeter of the Snow-Talon fire this made it a good candidate location for running DHSVM and looking at the response to fire.

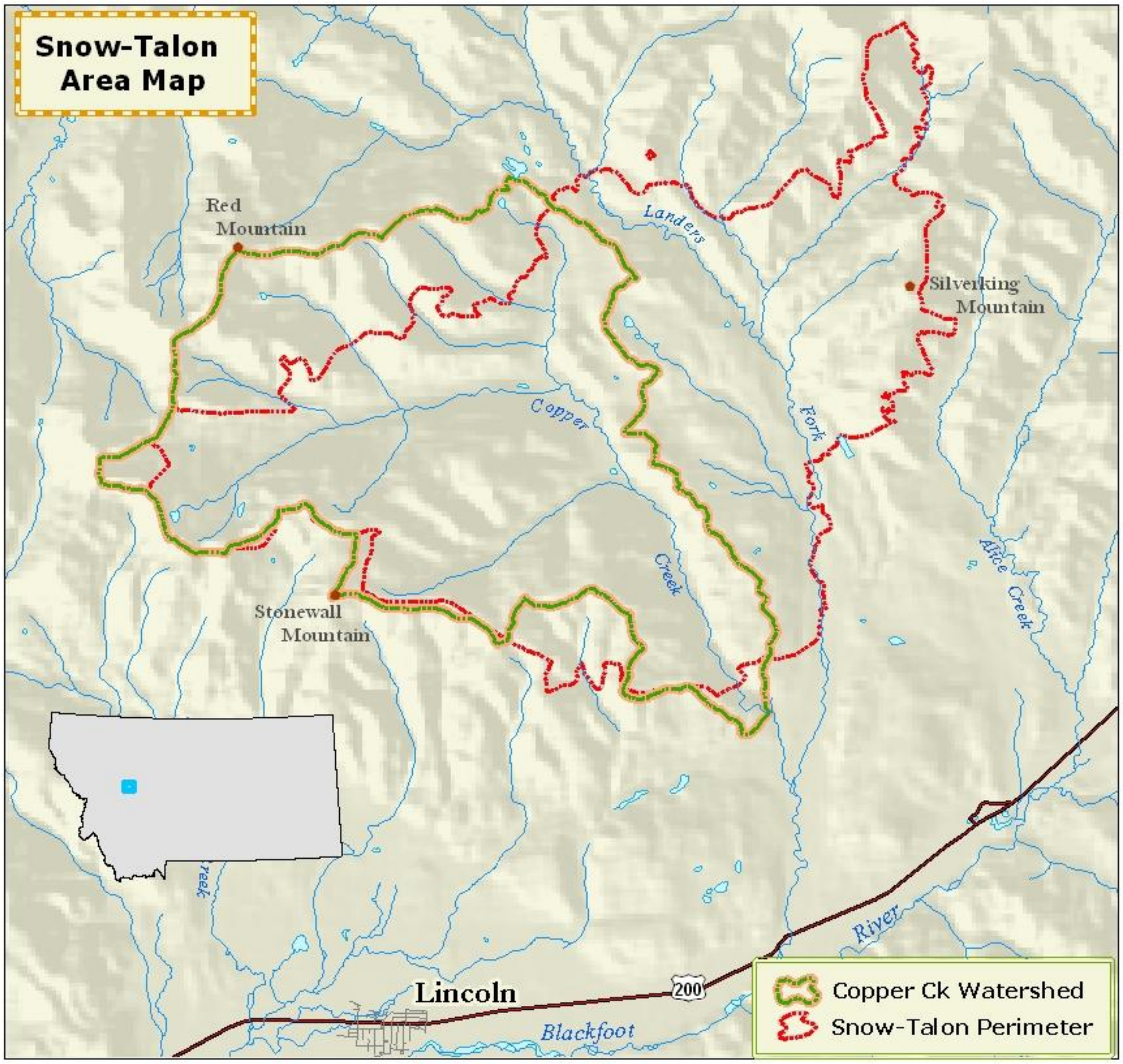

Figure 3 - Snow-Talon area map

Fire Severity, Soils, Vegetation, and Weather Data

Approximately 7284 hectares burned out of a total of 10,360 hectares contained within the Copper Creek watershed. Of the burned hectares, around 4856 hectares or 48% of the watershed was classified high-severity burn. This information was derived from a Delta Normalized Burn Ratio (ΔNBR) procedure (Key and Benson, 2003) performed with pre- and post-fire Landsat satellite imagery to identify different levels of burn severity. The dates of the pre- and post-fire images are 7/30/2003 and 10/2/2003 respectively. While the fire was not completely out at the time the entire portion of the fire within Copper Creek had already burned. These satellite images were also the best non-cloudy images that could be obtained around the time period. The availability of satellite data is determined by the Landsat passes as well as the weather at the time of the image. This is a rapid ΔNBR assessment as the images occur directly before and after the fire instead of a year after the start of the fire. The rapid assessment would be more feasible for addressing post-fire issues shortly following the end of the fire as this when the BAER report is being compiled. While a long term assessment might allow us to identify areas of enhanced re-growth and also distinguish between regions stressed by drought rather than fire, the timing necessary to obtain a BAER report would not make this method feasible. So the analysis only includes the short term assessment as to simulate what actually might have to occur if this process was repeated for a management application. The assessment is based in the differences in reflectance between healthy vegetation and burned regions. Landsat TM bands 4 and 7 which represent near infrared and mid-infrared respectively are used for NBR. Each satellite image is processed using the following equation:

$$NBR = \left(\frac{nearIR - midIR}{nearIR + midIR} \right)$$

Equation 1

Finally giving us ΔNBR:

$$\Delta NBR = NBR_{pre-fire} - NBR_{post-fire}$$

Equation 2

The images are then compared using the ΔNBR procedure by subtracting the NBR post-fire image from the NBR pre-fire image. This provides a theoretical range of ΔNBR values from -2000 to +2000 of which the extreme values of this range will most likely not be represented in typical ΔNBR analysis. These values can then be classified into varying levels of fire severity. In creating breaks for the Snow-Talon fire severity image, I utilized post-fire aerial photos taken of the area (Bassette, 2005). By overlaying the fire severity image over the photos I was able to identify areas of high, moderate and low severity. I felt this was a good way to identify the burn severity breaks due to the availability to high resolution aerial photos which are not often available. Table 1 represents the thresholds which I used.

Severity Class	ΔNBR value
0 - Unburned	< 250
1 - Low	250 – 375
2 - Moderate	375 – 575
3 - High	> 575

Table 1

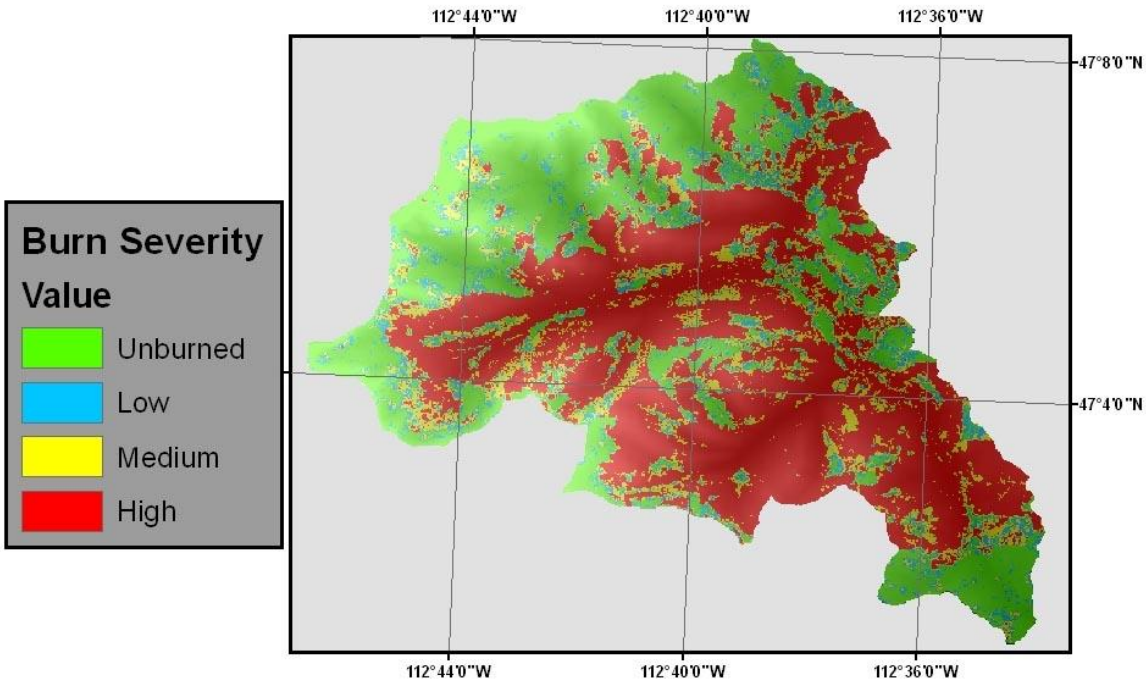

Figure 4 – Fire Severity

Limitations of the ΔNBR process can be found in looking how the image is derived. Because we are looking at the differences in live vegetation before and after the fire we are overlooking areas which may have not been healthy vegetation prior to the fire. Instances where this might occur include vegetation that is stressed due to drought. This was the case in the late summer of 2003 following many days with no precipitation. Areas burned in previous fires could also be overlooked due to the lack of healthy vegetation to compare to pre and post burn images. This may lead to incorrect assumptions about fires effects on the vegetation, duff and soil layers in these previously burned areas.

Due to the amount of high severity burn within the watershed, there was concern of higher peak flows, mass wasting, and erosion events (Stuart et al., 2003). Down stream risks such as flooding, undersized road culverts and potential damage to private property were assessed for Copper Creek (Stuart et al., 2003). Peak flows for Copper Creek were expected in the range of 18 to 35 cubic meters per second (Stuart et al., 2003).

The vegetation input layer was derived using Satellite Imagery Land Cover (SILC) classification data (Redmond, 1996). The layer was then reclassified to match a similar classification in the input file for DHSVM. The resulting vegetation types were deciduous broadleaf, mixed forest, closed shrub, grassland, bare, water, xeric conifer, mesic conifer, subalpine conifer, and alpine meadow. Refer to Table 2 and to Figure 5 for vegetation classification.

SILC ID	**SILC**	**DHVSM**
3150	Low/Moderate Cover Grasslands	Grassland
3170	Moderate/High Cover Grasslands	Grassland
3180	Montane Parklands and Subalpine Meadows	Grassland
3200	Mixed mesic shrub	Closed Shrub
3300	Mixed Xeric Shrubs	Open Shrub
4140	Mixed Broadleaf Forest	Deciduous Broadleaf
4203	Lodgepole Pine	Xeric Conifer Forest
4212	Douglas-fir	Xeric Conifer Forest
4223	Douglas-fir/Lodgepole Pine	Xeric Conifer Forest
4260	Mixed Whitebark Pine Forest	Subalpine Conifer Forest
4270	Mixed Subalpine Forest	Subalpine Conifer Forest
4280	Mixed Mesic Forest	Mesic Conifer Forest
4290	Mixed Xeric Forest	Xeric Conifer Forest
4300	Mixed Broadleaf and Conifer	Mixed Forest
5000	Water	Water
6110	Conifer Riparian	Mesic Conifer Forest
6120	Broadleaf Riparian	Deciduous Broadleaf
6130	Mixed Broadleaf and Conifer Riparian	Mixed Forest
6300	Shrub Riparian	Closed Shrub
6400	Mixed Riparian	Mixed Forest
7300	Rock	Bare
7500	Mines/Quarries	Bare
7800	Barren	Bare
8100	Alpine Meadows	Alpine Meadow

Table 2

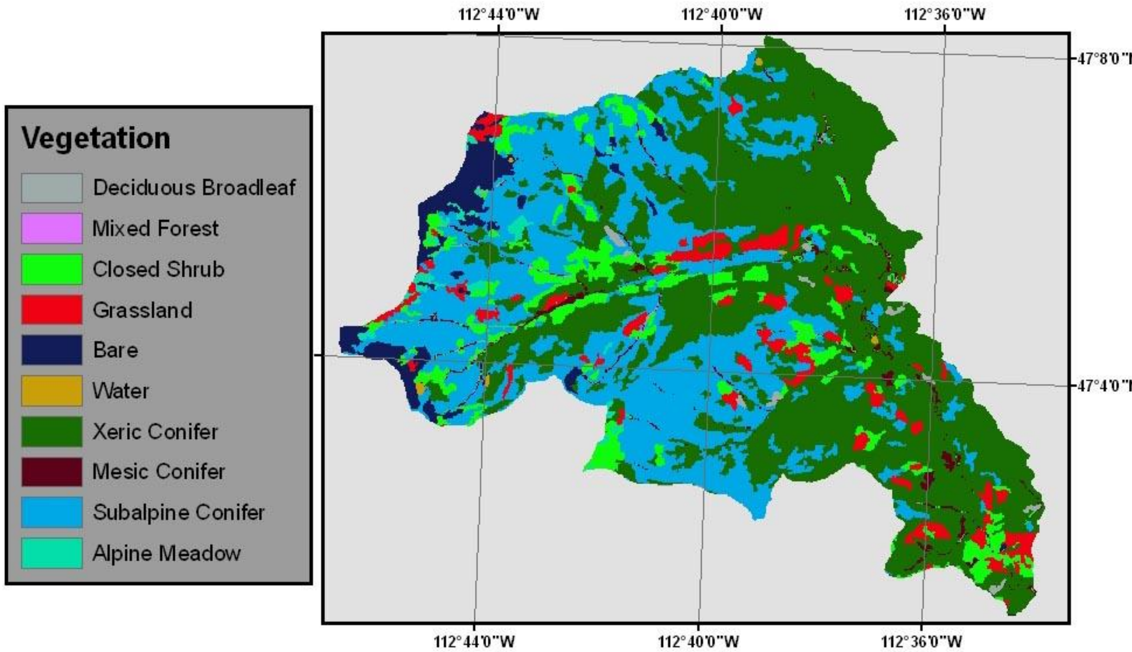

Figure 5 - Vegetation

Soils input data were derived from the Helena National Forest Land Type Characterization (Farley, 2003). Soils classification data were based on landform, geology, and slope gradient resulting in a soil texture (Farley, 2003). Soil texture is the required input into DHSVM. Small portions of soils data on private land and in the northeast portion of the watershed containing within the Scapegoat Wilderness were not available. Using the information the Helena National Forest Land Type Characterization on landform and slope gradient while also comparing nearby soils, the soil texture data for the wilderness and private land was extrapolated to provide a complete data layer. Soils data were then reclassified into the following soil texture groups sandy loam, silty loam, loam, water, and bedrock, which could then be assigned the appropriate hydrologic soil parameters in the DHSVM configuration file.

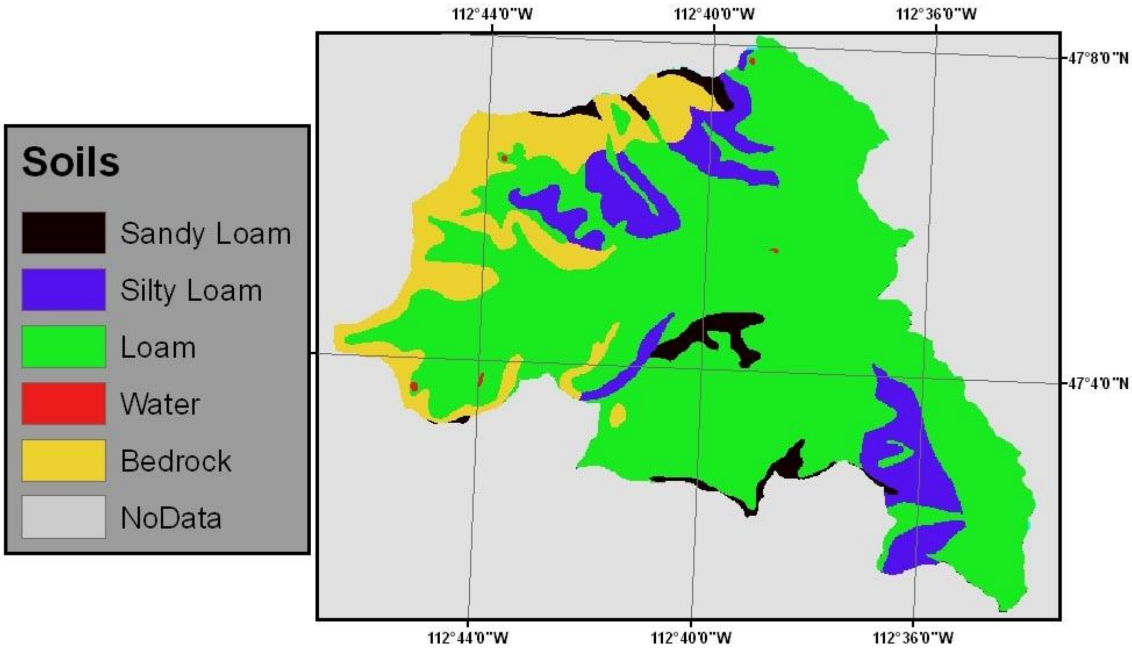

Figure 6 - Soils

For weather station data inputs, DHSVM requires an ASCII file containing model time step, air temperature, wind speed, relative humidity, incoming shortwave radiation, incoming longwave radiation, and precipitation. Weather station data or gridded weather data such as the Mesoscale Model (MM5) can be used as meteorology inputs(Lettenmaier, 2006). Within the Copper Creek watershed there are two Snowpack Telemetry (SNOTEL) stations, Copper Camp and Copper Bottom. The Lincoln Remote Automated Weather Station (RAWS) is located approximately five miles south of the Copper Creek watershed. I felt it was important to use this locally-measured weather station values in order to most accurately represent the meteorological conditions that occurred throughout my study period. It is not common to have this many weather stations available in a small Western Montana watershed. Substantial work with the weather data had to be done to take the SNOTEL and RAWS formats and convert them to the format required for DHSVM. Data required, but not available for the SNOTEL sites, included wind speed, short and longwave radiation and relative humidity. Missing values for the RAWS included longwave radiation. A wind model was not used to determine wind values, rather all wind values came from the Lincoln RAWS. Wind is a significant factor in snowmelt; due to good agreement in measured and modeled values for snowmelt in studies in British Columbia (Thyer *et al.*, 2004; Whitaker *et al.*, 2003) it was left to the distributed component of DHSVM (Storck *et al.*, 1998; Wigmosta et al., 2002) to adjust wind values spatially.

The Lincoln RAWS contained measured values for relative humidity. To estimate the relative humidity for the SNOTEL stations the assumption was made that because of the small spatial extent watershed that air masses entering the area would have similar water vapor characteristics throughout the range of the watershed. This assumption allows the calculation of the Actual Vapor Density from the measured Lincoln RAWS Relative Humidity (RH). The Saturation Vapor Density (SVD) can then be calculated using the temperate in degrees Celsius measured at the SNOTEL site with the following equation (Nave, 2005).

$$SVD = (5.018) + (0.32321 * SNOTELTemp) + 8.1847 * 10^{-3} * SNOTELTemp^{2} + 3.1243 * 10^{-4} * SNOTELTemp^{3}$$

Equation 3

The RH was then calculated using the assumed AVD calculated from the Lincoln RAWS station temperature and RH data along with the SNOTEL SVD in the following equation.

$$RH = (AVD / SVD) * 100$$

Equation 4

The variation for incoming shortwave radiation was expected to be small considering the small spatial extent of the modeled area. The shortwave radiation values measured by the Lincoln RAWS were also used for all stations in the study area. To derive a longwave radiation parameter, an R-squared correlation of 0.899 was established between measured longwave radiation values and shortwave radiation and temperature from a DHSVM project in the Entiat River basin in north central Washington state. The resulting regression equation was used to calculate the longwave radiation values for all three stations.

$$Longwave\_Radiation = Temperature(4.353) + Shortwave\_Radiation(-.0254) + 272.348$$

Equation 5

SNOTEL precipitation data also presented problems as it had accumulated values for each time-step with corrected values only occurring at midnight of each night. This meant that the fluctuations of the instruments during the day may incorrectly look like precipitation accumulation (Ward, 2005). I developed rule-based system to attempt to identify times of actual precipitation accumulation as opposed to when it was just instrument fluctuations. The basic rules are as follows:

1. Total accumulations can not exceed the accumulated values defined by subtracting last nights corrected value from the following midnight correct value.

2. Fluctuations in a positive or negative direction followed by just the opposite fluctuation would be considered instrument fluctuations.

3. Consecutive time periods with precipitation were given precedence because it was felt that it more likely represented a precipitation event rather than a single instrument fluctuation.

Because the SNOTEL data were recorded in three-hour increments, this is the time interval at which DHSVM will run. Due to the large number of weather data records, data calculations were made using Microsoft Visual Studio 2003 connecting to an Access database and coded in Visual Basic .NET.

Known failure locations

Within Copper Creek watershed the highest number of erosion events following the Snow-Talon fire occurred during a high intensity rainstorm on August 19th 2004. The Copper Bottom SNOTEL station recorded one centimeter of rain in the 2 days prior to 19th followed by 1.6 centimeters of rain within a 3 hour period. This was on top of bare soils already wet from previous storms. In one location the road was covered in mud and rocks while Copper Creek and several tributaries were muddied (Kamps, 2005). Two regions with known high landslide potential were identified by the BAER report on the North Fork of Copper Creek (Stuart et al., 2003). There were no reported failures at those locations. Other regions of high erosion potential are noted in red with moderate erosion potential shown in orange in Figure 6.

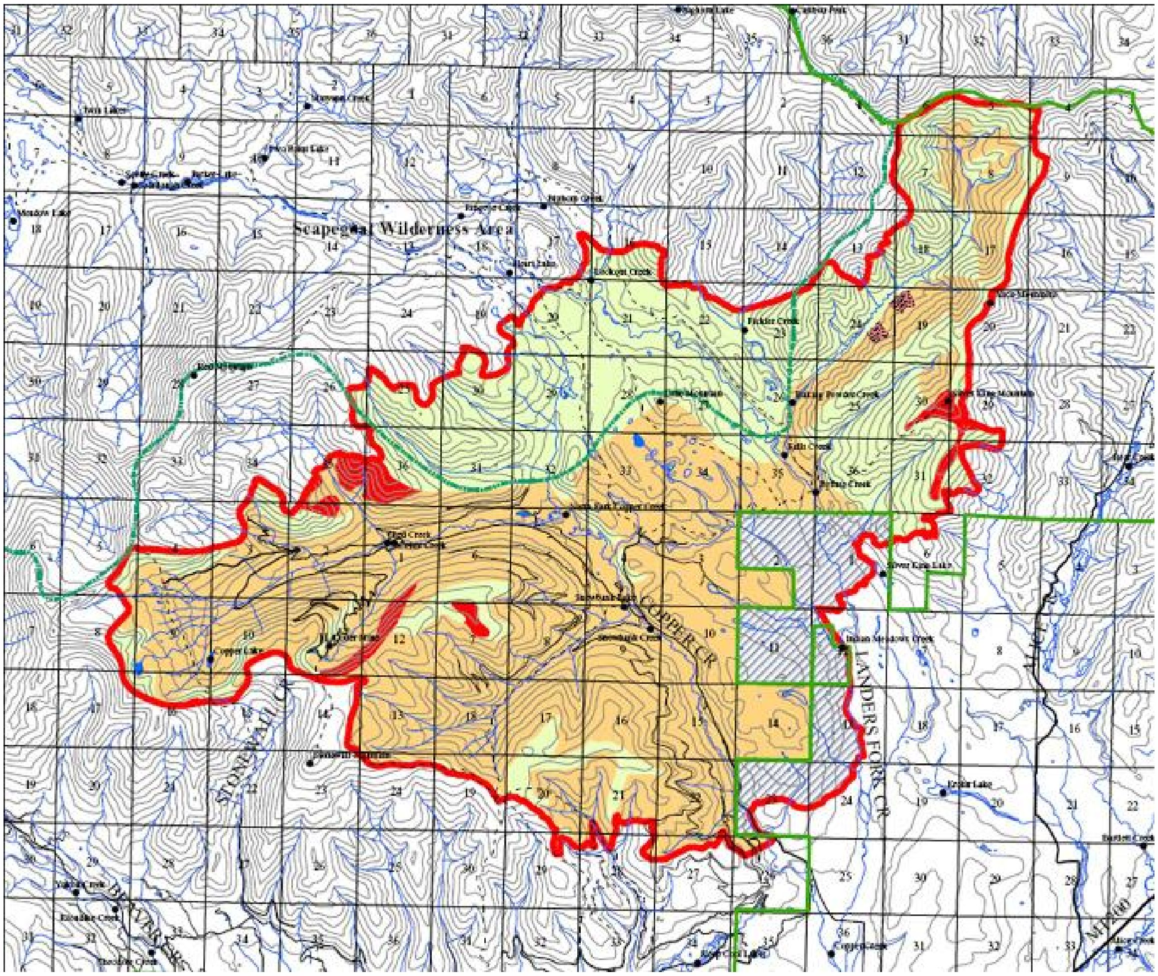

Figure 7 **Soil Erosion Potential – BAER**

(Stuart et al., 2003)

Chapter 3: DHSVM Calibration

To better understand how DHSVM would perform with the Copper Creek watershed data layers, modeled hydrograph results using historical weather data were compared to two gauged sections of the Blackfoot River monitored between 1968 and 1975. The United State Geological Survey (USGS) gauged a 39 square mile section of the Blackfoot river from 1968 to 1970 and then placed the gauge further downstream, past the confluence of Alice Creek, encompassing a total of 251 square miles from 1971 to 1975.

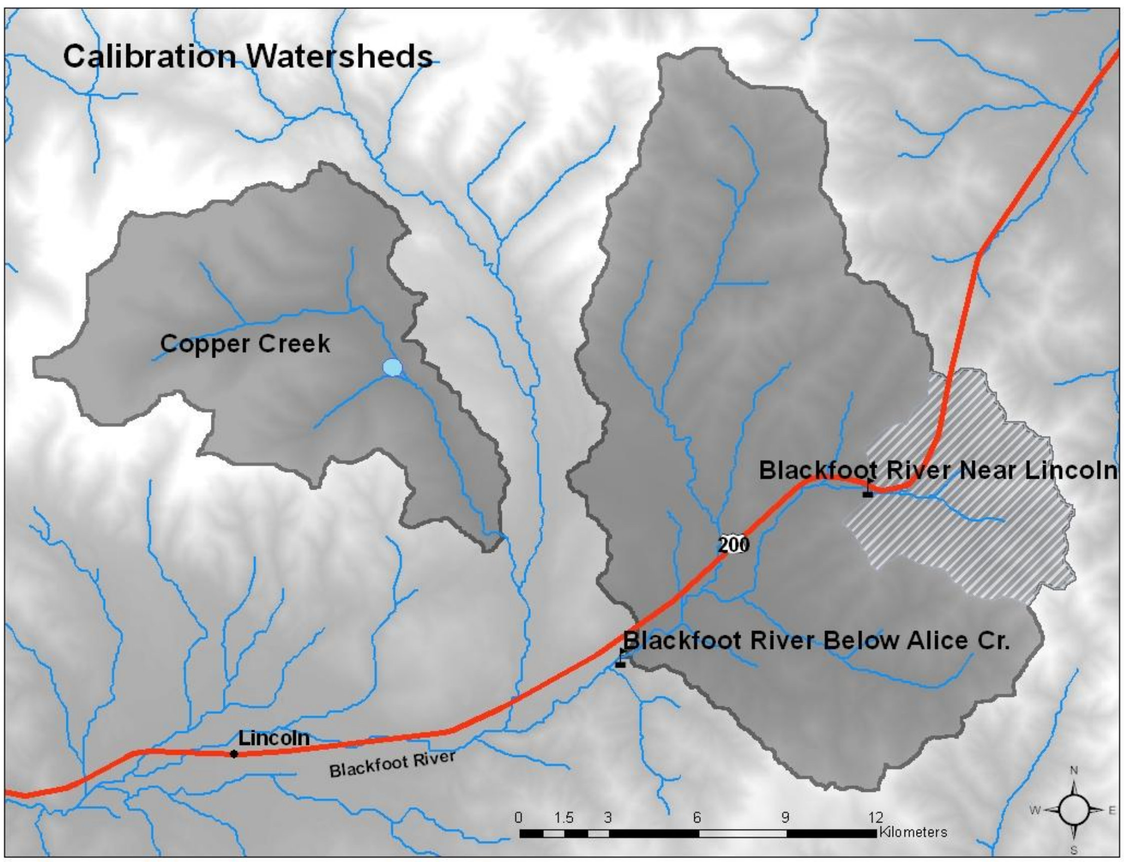

Figure 8 – Calibration watershed and gauge locations

Calibration Watershed Comparison

Site Name	USGS Gauge #	Outflow Elev (M)	Drainage Area km^2	Latitude	Longitude	Avg. Flow M^3/S
Blackfoot R. near Lincoln MT	12334600	1563	39	47.0436	-112.4038	0.46
Blackfoot R. bl Alice Cr nr Lincoln MT	12334650	1463	251	46.9892	-112.5111	2.21
Copper Creek	modeled	1518	104	47.0245	-112.5657	1.24*

* Average flow from DHSVM modeled data.

Table 3

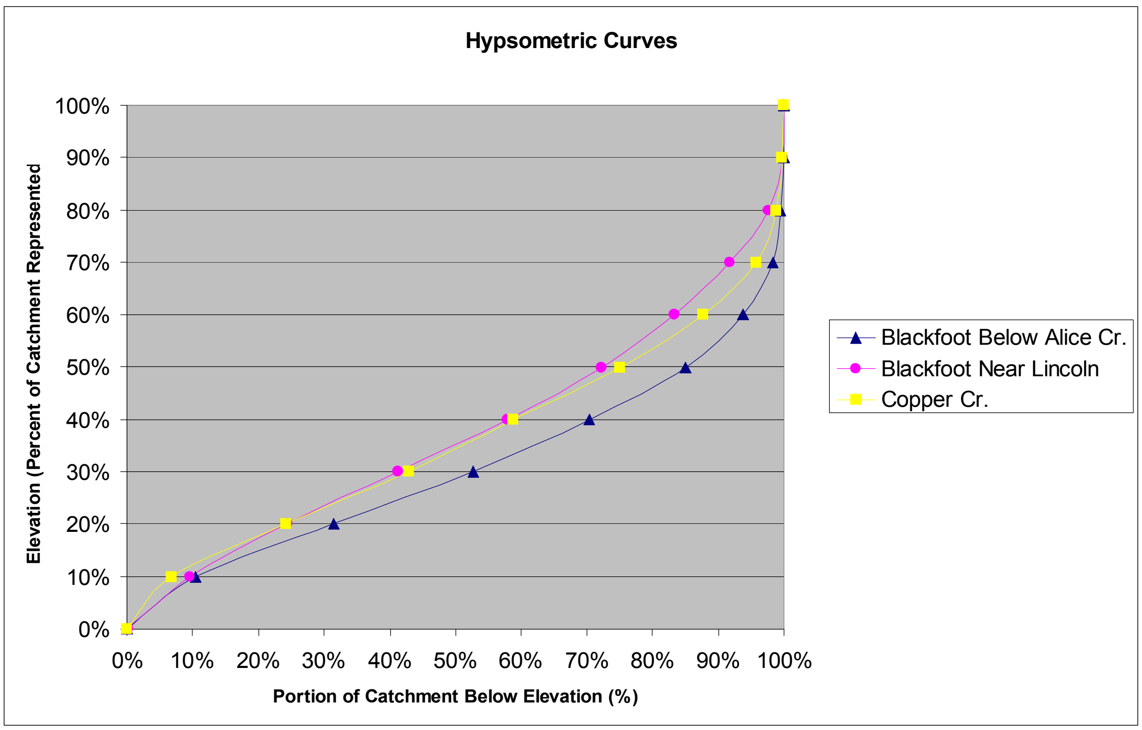

Figure 9

The hypsometric curves in Figure 9 represent the proportion of land area within the watershed at a particular elevation. The purpose of looking at the location, size, elevation characteristics were intended to establish the relationship between the 3 different watersheds. It was important to show that the watersheds were similar in shape, composition and location to make the assumption that they would have similar hydrologic responses. The largest differences between the watersheds were there size. From these differences in size we could expect the response of the Copper Creek (104 km^2) watershed to have a response in between that of Blackfoot near Lincoln (39 km^2) and the Blackfoot below Alice Creek (251 km^2) gauges. Because of the close proximity of all the drainages as well as similar vegetation the modeled outflow of peak runoff, storm runoff and base flow for Copper Creek would be expected to fall in between that of Blackfoot near Lincoln gauge and Blackfoot below Alice Creek gauge.

Historical weather data was derived from data from the Lincoln Ranger Station RAWS, Rogers Pass weather station, Helena Airport weather data, National Climate Data Center (NCDC) and the USDA Solar Calc solar radiation estimation application (Spokas and Forcella, 2006). The combination of weather data was used to extrapolate weather data to the current location of the Copper Camp and Copper Bottom SNOTEL locations. The only data available in three hour increments from the Lincoln Ranger Station RAWS was temperature. Wind was averaged by month; precipitation and relative humidity were averaged by day. Incoming solar radiation was calculated using Solar Calc based on day of year, precipitation, minimum and maximum temperatures. Long wave radiation was calculated from equation 5 used in chapter 2.

When the model was run with the historical weather data and derived soil and vegetation raster data the assumption was that the peaks would coincide due to the similar weather in the region while the magnitude of those peaks would fall in between that of the 39 and 251 square kilometer drainages. Copper Creek watershed is approximately 104 square kilometers in area. Figure 10 below shows the two measured watersheds with the modeled Copper Creek data. The left blow-up shows Copper Creek modeled data compared to Blackfoot near Lincoln measured data. On the right modeled Copper Creek data is show with measured data of the Blackfoot below Alice Creek.

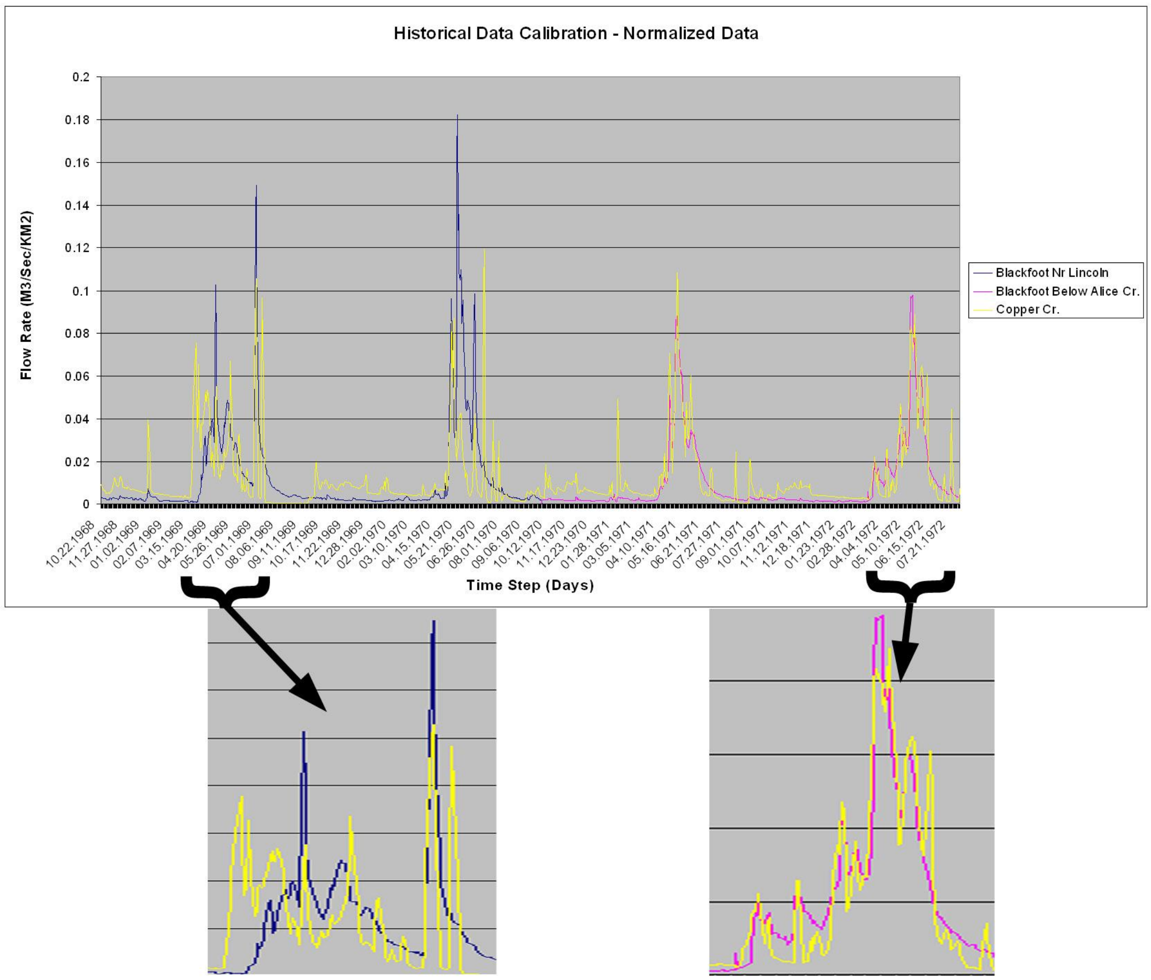

Figure 10 – Historic streamflow calibration graph (with sections enlarged)

To establish the how well the model results match that of the two comparison watersheds a Nash-Sutcliffe efficiency coefficient (Nash and Sutcliffe, 1970) was run on the normalized measured output and the DHSVM modeled output to establish the how well the modeled results explained the measured flows.

$$E = 1 - \left(\frac{\left(\sum_{t=1}^{T} \left(Q_0^t - Q_m^t\right)\right)^2}{\left(\sum_{t=1}^{T} \left(Q_0^t - \overline{Q_0}\right)\right)^2} \right)$$

Equation 6

Where Q^0 is observed stream flow, and Q_m is modeled stream flow. Q^t is stream flow at time t.

Copper Creek modeled data and observed data from the Blackfoot near Lincoln gauge resulted in an efficiency coefficient of 0.29 while Copper Creek modeled data compared to observed flows at the Blackfoot below Alice Creek gauge had an efficiency coefficient of .81. The efficiency coefficient of .81 indicates that the model is predicting the measured data very well for the Blackfoot below Alice Creek, while a value of .29 indicates the model is less able to explain the variance seen in the measured values of the Blackfoot near Lincoln watershed. The low value of .29 for the Blackfoot near Lincoln watershed may be due to the small size of the watershed. These efficiency coefficients can be thought of as very similar to that of an R-Squared value in that the close the value is to one, the better the model is able to represent the data.

Chapter 4: DHSVM Mass Wasting and Fire Disturbance Components

Erosion and sediment transport along with a disturbance component have been added to the original DHSVM model (Doten et al., 2006; Lanini and Lettenmaier, 2005). These additional components made it possible to attempt to model the hydrologic effects of wildfire on soil. On a user-defined date, sometime close to when the actual fire took place, the disturbance component alters vegetation based on a fire severity input layer. The mass wasting component of the sediment erosion and transport model also runs on specific defined dates typically where precipitation levels are highest.

Fire Disturbance Module

The removal of vegetation following fire will reduce transpiration while increasing soil moisture. By removing the organic material at the surface, the soil is now exposed to raindrop impact and increased potential for overland flow. Depending on vegetative material and fire severity, hydrophobic conditions can also occur, reducing the infiltration rates (DeBano, 1998). Root cohesion of the soil is reduced with plant mortality. The DHSVM fire disturbance module (Lanini and Lettenmaier, 2006) alters model parameters, leaf area index, root cohesion and vegetative surcharge to represent vegetative mortality and regeneration. Alteration to the vertical soil infiltration capacity parameters represents the affects of hydrophobicity. Changes in root cohesion are determined in the model by the following four assumptions:

1. Low intensity fire has complete mortality for understory and no overstory mortality.
2. Medium intensity fire has complete understory mortality and 50% overstory mortality.

3. High intensity fire results in complete mortality of both understory and overstory.

4. DHSVM does not differentiate between understory and overstory root cohesion.

The DHSVM fire disturbance module was originally developed for the Cascades region. Therefore two region specific assumptions were made: first, because salvage logging is a common in the Cascades, dead trees are removed and there is no decrease in vegetation surcharge; second, based on a study by Dyrness (1976), hydrophobic conditions last up to six years. The fire disturbance model also assumes recovery of Leaf Area Index (LAI) in ten years while complete overstory LAI requires 25 years to return to pre-disturbance levels. With the Snow-Talon simulation only lasting 2 years, LAI return was determined not to be a significant factor.

Sediment Erosion and Transport Module

The four components of the sediment module are: mass wasting, hillslope erosion, erosion from forest roads and channel-routing algorithm. The sediment module output is determined by the following temporal and spatial outputs of DHSVM: depth to saturation, saturation and infiltration excess runoff, precipitation, leaf drip and channel flow. (C.O. Doten and Lettenmaier, 2006) Of the four components I will be focusing on the stochastic mass wasting calculations to predict slope failure following fire.

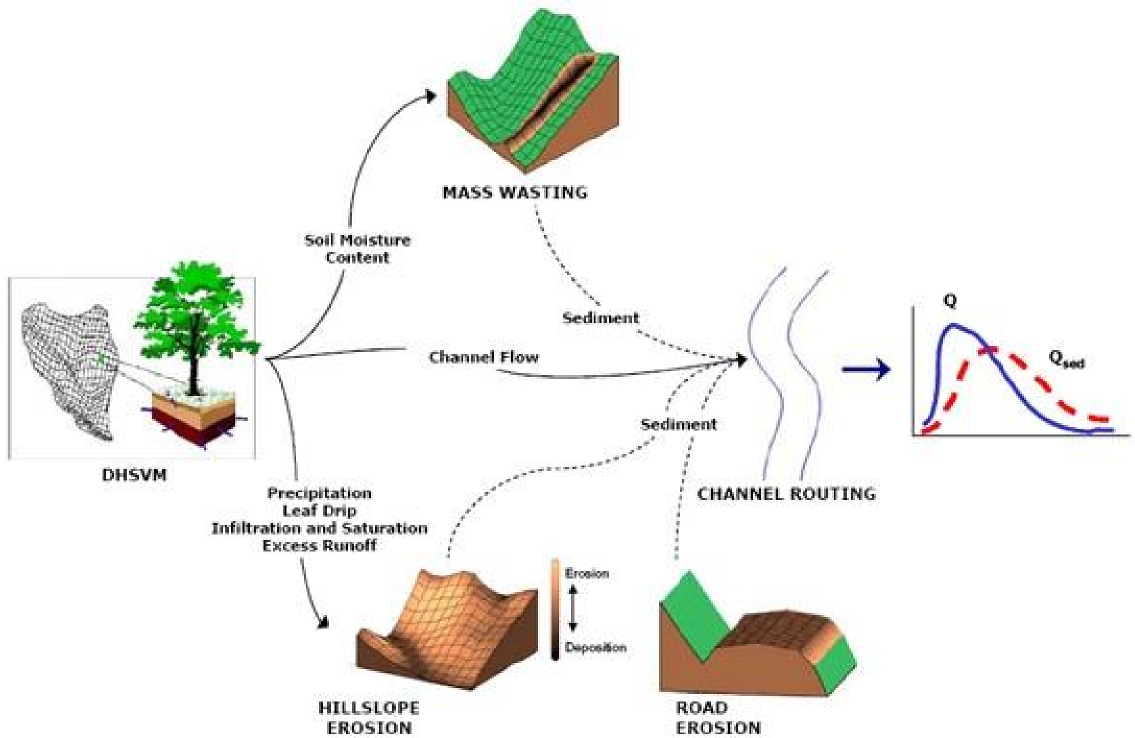

Figure 11

(C.O. Doten and Lettenmaier, 2004)

The objective of the mass wasting algorithm is failure prediction and downslope redistribution. The component runs for the number of iterations defined in the input file, which results in a probability of failure. A higher resolution DEM than that used in the DHSVM run is commonly used for mass wasting calculations. Only pixels that have soil and a slope greater than 10º will be included in the Factor of Safety (FS) analysis. The FS equation is described by Doten (2004) as it relates specifically to DHSVM.

$$FS = \left(\frac{resis\tan ce\ of\ soil\ to\ shearing}{downslope\ component\ of\ soil\ weight} \right)$$

Equation 7

$$FS = \frac{\left(\frac{2(C_s + C_r)}{\gamma_w d \sin(2S)} + \frac{(L - m)\tan\phi}{\tan(S)} \right)}{L}$$

Equation 8

where:

$$L = \left(\frac{q_0}{\gamma_w d} \right) + m\left(\frac{\gamma_{sat}}{\gamma_w} \right) + (1 - m)\left(\frac{\gamma_m}{\gamma_w} \right)$$

Equation 9

and C_s is the effective soil cohesion, kg/m^2; Cr is the root cohesion, kg/m^2; m is the relative saturated depth (dimensionless); φ is the effective angle of internal friction of soil on impermeable layer; γ_w is the weight density of water, kg/m^3; d is the soil depth above failure plane, m; S is the surface slope; q_0 is the vegetative surcharge per unit plan area, kg/m^2; γ_{sat} is the weight density of saturated soil, kg/m^3, and is determined from the average bulk density of all soil layers (required input for DHSVM); and γ_m is the weight density of soil at field moisture content, kg/m^3 (Doten and Lettenmaier, 2006).

Pixel failures are represented by an FS value less than one. By using a probability distribution of either normal, triangular, or uniform stochastic results are generated using parameters defined in the sediment input file. There are four input parameters for shear strength and loading: soil cohesion, angle of internal friction, root cohesion and vegetation surcharge. Once a pixel has failed, that material is routed downhill towards the steepest decent. Failure probability is then calculated for the pixel where the deposition occurred, either moving material downslope or stopping at a stable pixel or stream network. Soil stability calculation framework for DHSVM are partially derived from the Level I Stability Analysis (LISA) model (Hammond et al., 1992) as well as the SHETRAN/SHESED modeling system (Wicks and Bathurst, 1996) which uses mass failures and rule-based redistribution of sediment.

Several maps can be output from DHSVM at defined time-steps. When a probability of failure map is produced, a binary raster map is created containing float values from zero to one representing pixel failures. A text summary of the number and distribution of failures is also generated.

Chapter 5: DHSVM Model Runs on Copper Creek Watershed

Three different DHSVM scenarios were run on the Copper Creek watershed. First I looked at a DHSVM model run without a fire disturbance to simulate what slope failures and streams flows could be present under conditions prior to the fire. Second, the model was run with the fire severity layer as input into the fire-disturbance module to represent the Snow-Talon fire event. Third, a design storm representing two inches of rain over a six hour period was used to simulate expected 100 year, six hour precipitation intensities. Figure 12 below represents isopluvials of 100 year six hour precipitation in tenths of an inch. Red Mountain is at the northwest corner of the Copper Creek watershed. A design storm is a common way for managers of a post-fire assessment to understand the potential hydrologic affects on stream flows and erosion.

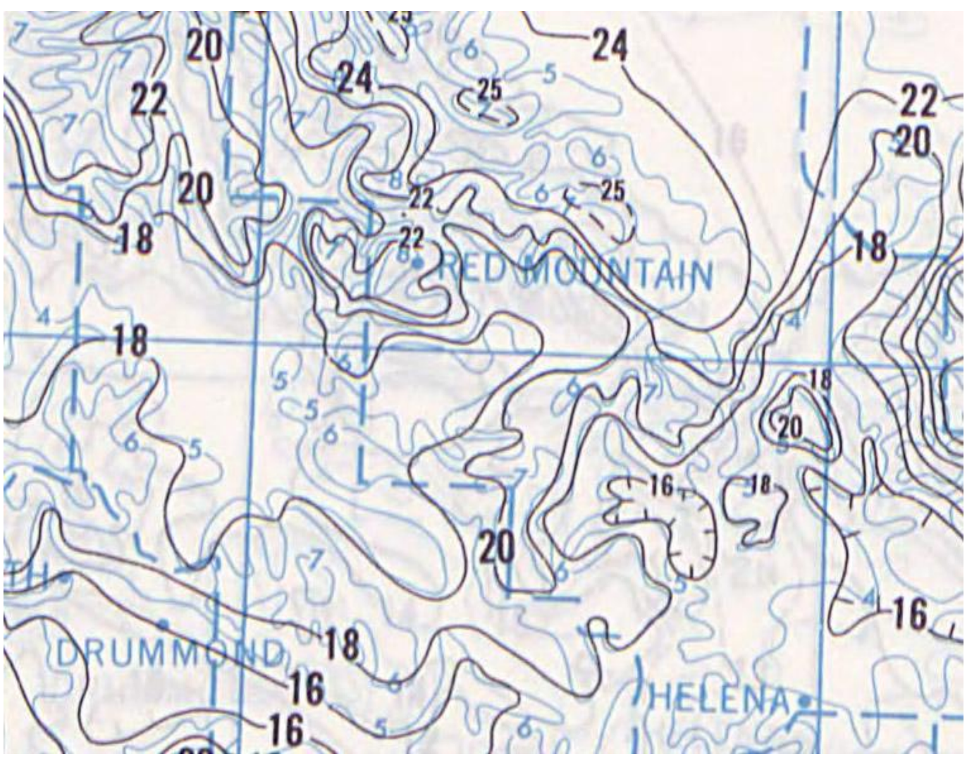

Figure 12 - Isopluvials of 100 year precipitation events over 6 hours measured in 10ths of inches.

(U.S. Department of Commerce, 1973)

DHSVM model runs were executed on a Dual 3.2Ghz Xeon server running, Linux RedHat Enterprise Advance Server 4 with 4GB RAM. A single run was from June 1, 2003 until January 31, 2004 with 8 time-steps per day due to 3 hour increments of weather data. The basin area consisted of 256,056 thirty meter pixels. A model run took approximately 3 hours and 22 minutes to complete.

Analysis and Results

Throughout this thesis, I have examined some of the known contributing factors to slope failure from previous studies, as well as some of the tools involved in identifying slope failure. After running DHSVM on the 2003 Snow-Talon fire, model output can be compared to a few known failures as well as to conclusions made by the BAER team. Results can be examined to understand correlations between the data input as well as the underlying physical equations driving the model. The three scenarios of no disturbance, fire disturbance, and design storm, allow for differences to be identified in the many user-defined outputs from DHSVM. Initially the objective was to identify regions of potential soil failure. DHSVM outputs maps derived from the calculations made using the MWM depict pixel failures with a value from zero to one. These binary file formats were then converted to ESRI GRID format so that the layers could be viewed in ArcMap. Failure probability ranged from 0 to 60%. The following maps depict probability of failure for each of the three scenarios.

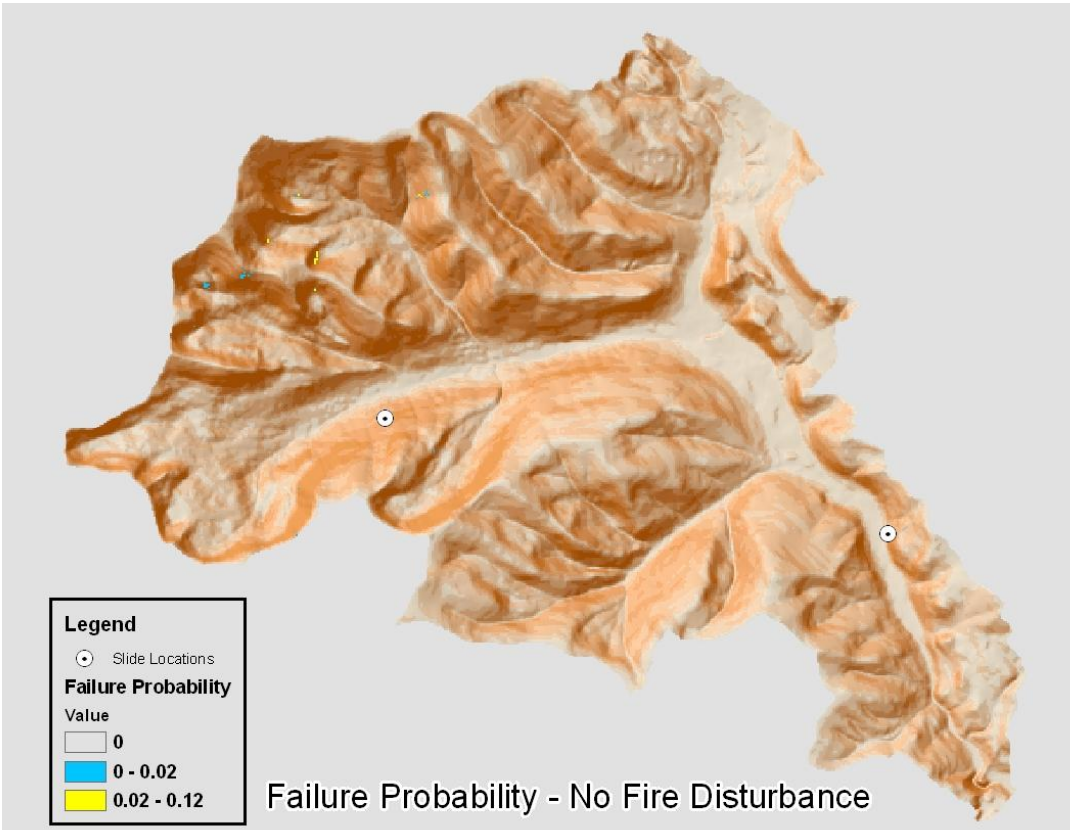

Figure 13 – Failure probability with no fire disturbance

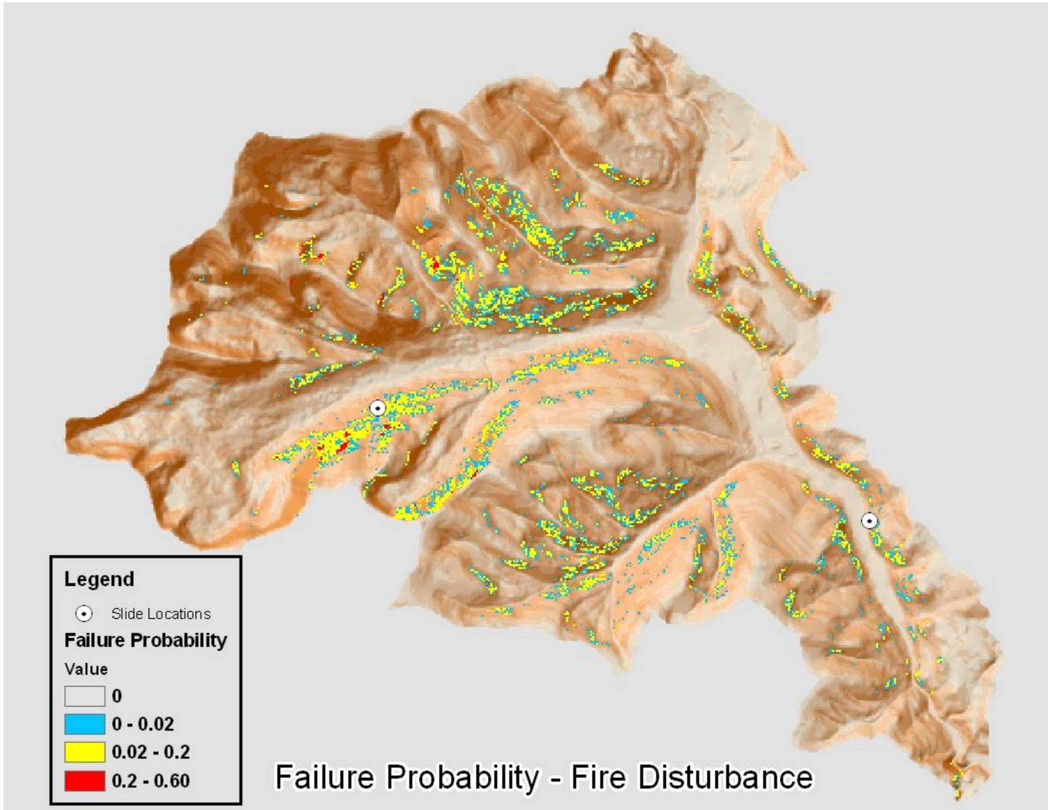

Figure 14 – Failure probability with fire disturbance

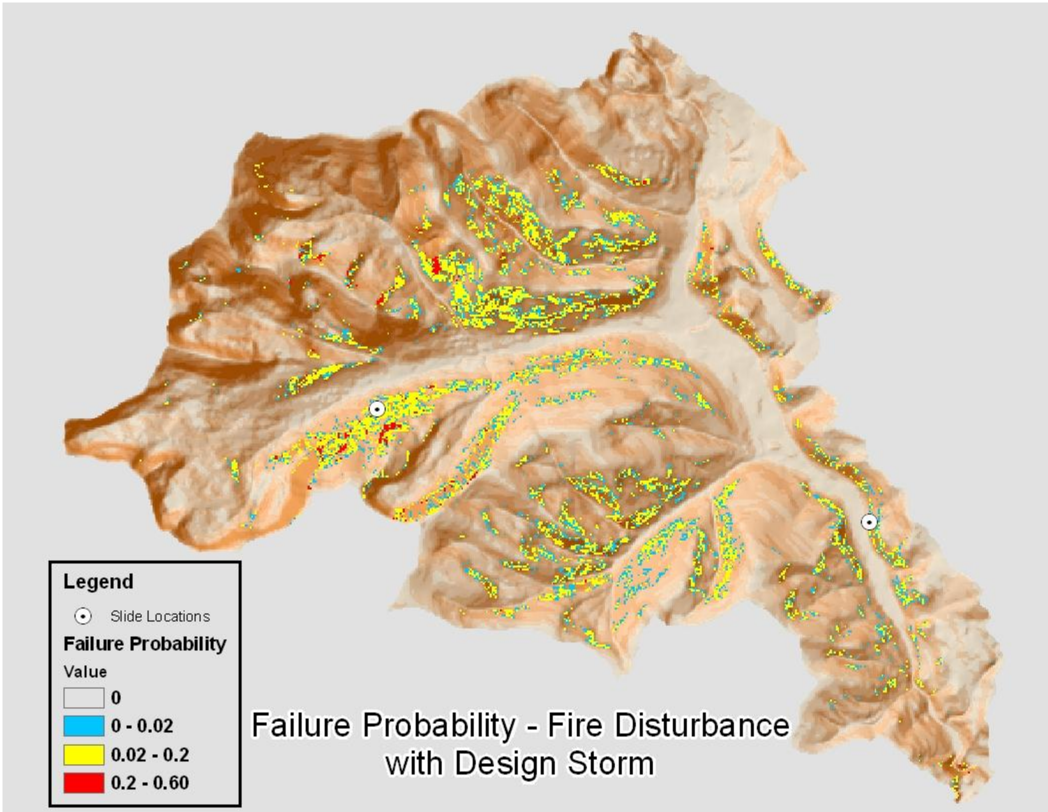

Figure 15 – Failure probability with fire disturbance and design storm

In figures 14 and 15 a close up of the upper and lower failures respectively can be seen in relation to the individual pixel failure probabilities. In figure 15 the proximity of the failures to the road caused the road to be closed due to debris and a culvert to be rebuilt and stabilized.

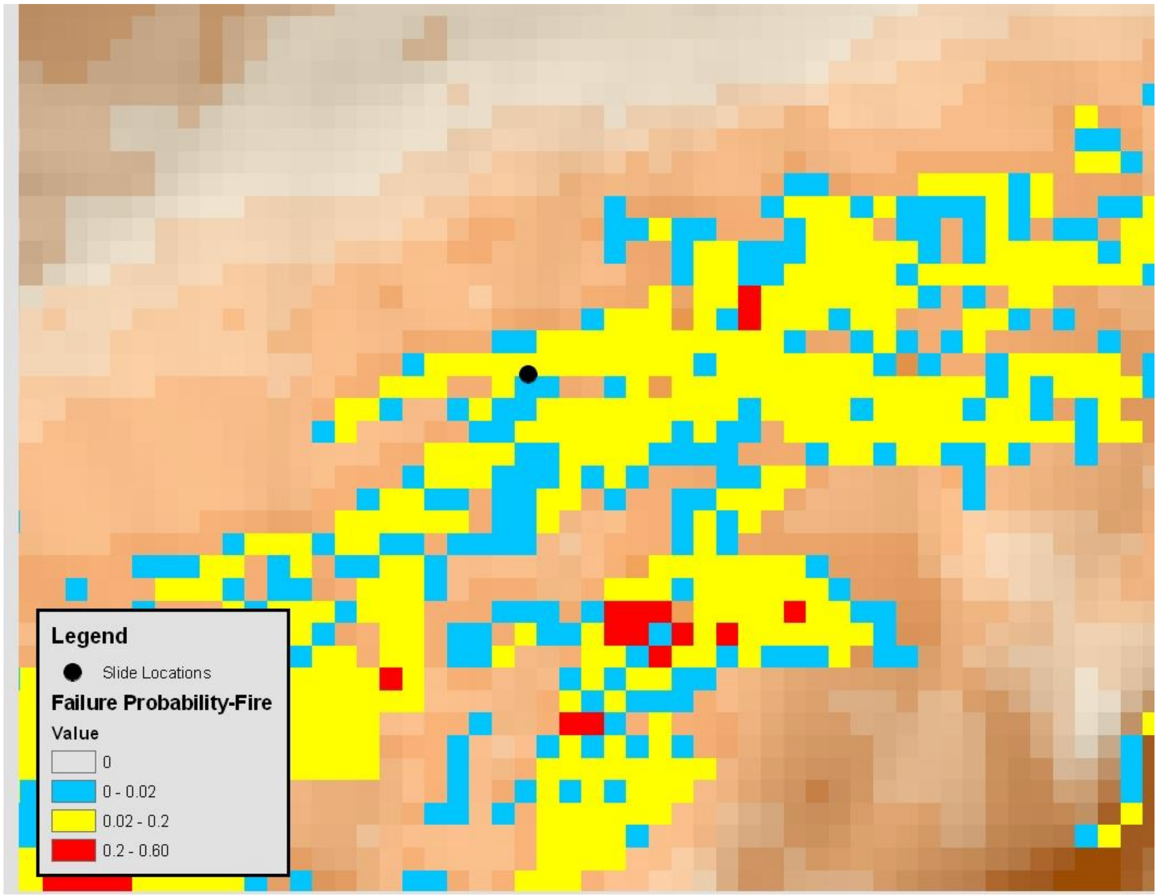

Figure 16 – Slide location 1 (Enlarged)

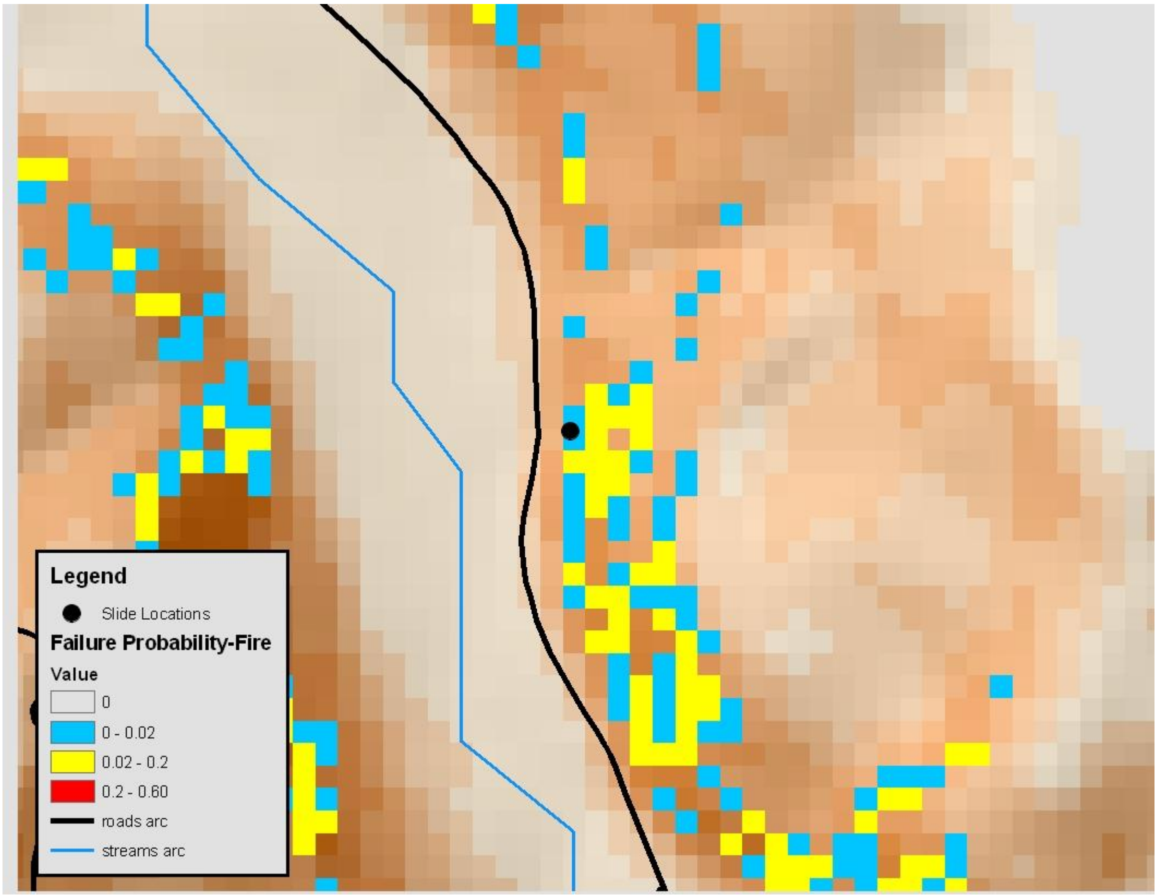

Figure 17 - Slide location 2 (Enlarged)

Soil Saturation

The amount and depth of water that exists in the soil profile an influencing factor in soil stability. Soil saturation is also the driving component for the MWM. The following images were produced for the August 19th 2004 rain event. For the first image saturation depths are much deeper over the entire Copper Creek watershed. The outline of this matches the area which was burned by the Snow-Talon fire. The image on the right shows much shallower saturation depths. Vegetation and soil types are influencing the differences in saturation levels without fire.(Neary et al., 2005b) Many of the lighter patches seen correspond to regions of grassland where the vegetative cover is less.

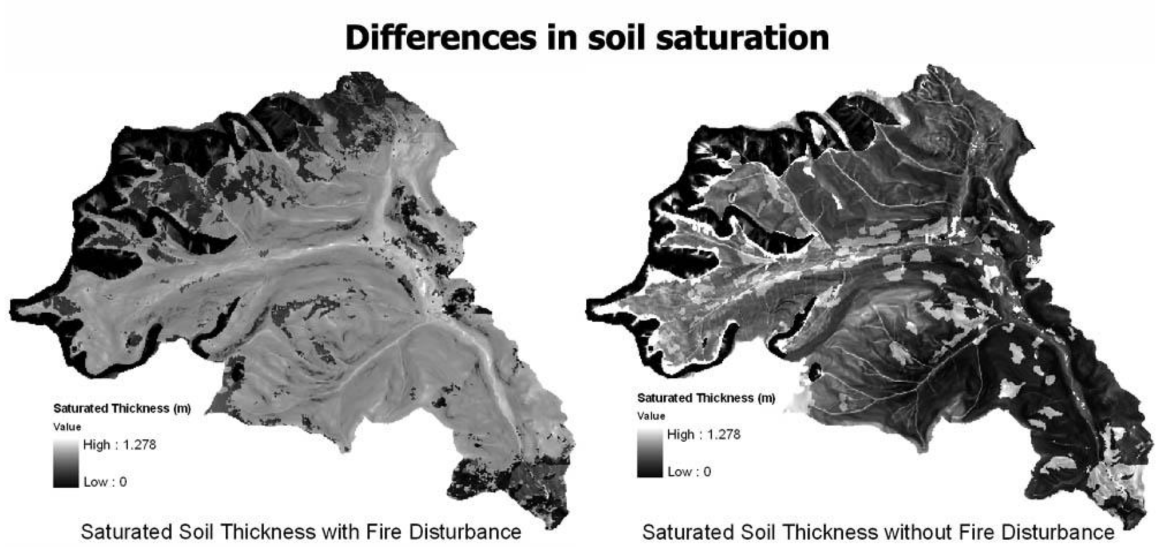

Figure 18 – Differences in soil saturation

Stream Flow

The influence of a disturbance is often quantified by the increase in stream run off. DHSVM produces an output of stream flow for every time step set in the configuration. Figure 19 shows modeled stream flow from 2003 to 2005 for both fire disturbance and no disturbance.

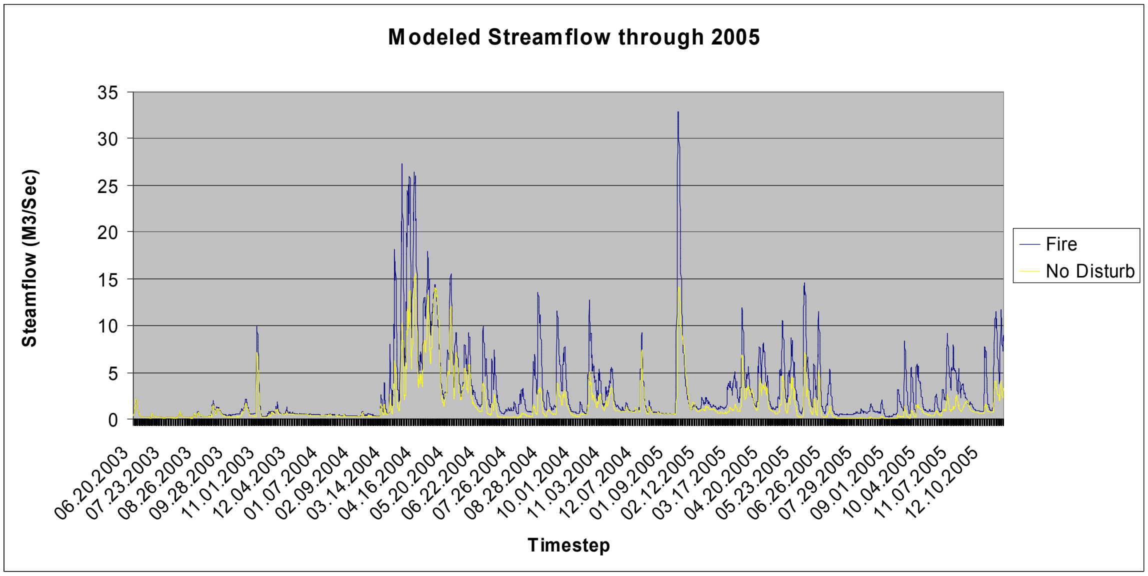

Figure 19 – Modeled Streamflow through 2005

Following the fire disturbance, modeled streamflow increased 53% in 2004-2005 compared to the model run with no fire disturbance. Peak spring runoff flows reached approximately 27 cubic meters per second. The design storm of 2 inches of rain over 6 hours produced modeled flows similar to that of modeled spring runoff. With the reduction of the vegetation following the fire in 2003, stream flows had a tendency to spike much higher than previous to the disturbance. Tables 4, 5 and 6 shows the differences between the model run with the simulated Snow-Talon Fire disturbance and without. Over the time period of 2004 to 2005 peak flows increased 61%, total water yield increased 52% and base flow increased 41%.

Peak Flow Yield (M^3/Timestep) April 1 to July 1

Year	Fire	No Fire	% Increase
2004	6379.31	4249.20	66.61%
2005	2903.93	1414.85	48.72%
Total	9283.24	5664.06	61.01%

Table 4

Total Water Yield (M^3/Timestep)

Year	Fire	No Fire	% Increase
2004	11381.72	6525.07	57.33%
2005	8750.56	3999.07	45.70%
Total	20132.28	10524.15	52.28%

Table 5

Base Flow Change (M^3/ Timestep) August 1 to January 30

Year	Fire	No Fire	% Increase
2004	3279.55	1574.55	48.01%
2005	3056.58	1021.05	33.40%
Total	6336.14	2595.60	40.97%

Table 6

Chapter 6: Conclusions

Overall water yield and peak flow discharge can substantially increase following fire. The flashiest response and highest peak flows are commonly found in smaller watershed 1 km^2 in area (Neary et al., 2005b). Based on simulated flows, the Copper Creek watershed at 104 km^2 showed peak flow increases up to 66% from simulations with no fire disturbance. Total water yield increased 52% and base flows increased 41% in 2004 and 2005. Without having measured flows the magnitudes can only be speculated upon based on observed damages due to peak flows. The August 19, 2003 rainstorm was the only event that produced a few localized areas of damage to the road and culverts. Several orders of magnitude increases in peak flow are not as common in Western Montana as they compared to large magnitude increases in the Southwestern United States (Neary et al., 2005b). Peak flows were found to be over estimated by DHSVM in a similar study done in the Entiat Experimental Watershed by Jordan Lanini of the University of Washington. Peak flows in this study were suspected to be greater than measured flows due to the uniform spatial extent of hydrophobicity applied by the fire module logic within DHSVM (Lanini, 2005).

The utilization of DHSVM for assessing soil failure probability combined the use of fine resolution soils, vegetation, elevation, and fire severity data with weather data at three hour increments. The objective was to see if results would allow us to more specifically identify areas of higher failure probability. While looking at soil failure it also gave the opportunity to look at the effects of different parameters at small spatial scales. The ability to run a simulation with weather data at shorter three hour increments, made it possible to look at the effects of short duration high intensity storms on both streamflow and soil failures. While DHSVM is still a research model with lengthy data preparation and parameterization, this use of DHSVM on fire may indicate its usefulness in management applications. There is a need to more specifically identify locations of potential failure following recent large wildfires to assist with the BAER team processes (Robichaud, 2005).

BAER Report Comparison

Shortly following fires such as the Snow-Talon fire, a BAER report is put together to assess immediate risks associated with burned area and suggest ways to mitigate such risks. The changes in hydrologic response of the watershed comprise a portion of this report as they pose flooding and mass wasting potential. Fire severity for the BAER report was derived by using aerial photographs and digitizing the hand drawn perimeters. I derived fire severity using ΔNBR using pre and post-fire Landsat TM images. A significant difference was in the area estimate of high severity burn. Often estimates derived from aerial sketch maps of fire severity can over estimate high severity burn regions. The BAER report had 62% high severity compared to 48% high severity which I had derived. For the ΔNBR technique to be used a clear post-fire Landsat image must be used which may not always be feasible with time constraints for completion of the report. Stream flow estimate in the BAER report estimate peak flows in Copper Creek to range from 15 to 31 cubic meters per second (Stuart et al., 2003). This matches well with DHSVM output estimating peak spring flows around 28 cubic meters per second and the design storm producing a peak of 27 cubic meters per second of flow. There were no available measured streamflow values for Copper Creek.

The Snow-Talon BAER report derived soil erosion hazards from burn severity mapping and erosion hazard assessments. 7689 hectares and 348 hectares were giving soil erosion ratings of moderate and high respectively. Areas of soil failure were then broken down into polygons of high medium and low soil erosion potential. DHSVM's soil erosion module predicted a total of 741 hectares with a probability of failure ranging from 2% to 60% for the fire disturbance scenario. Failures were depicted by a single 30 meter by 30 meter pixel. The results were specific regions on the hillslope where all factors modeled reached the failure threshold. Only a few areas of known failures locations were compared and the actual effectiveness of the failure prediction regions leaving that portion of results not quantified. Of the two known slide locations, both fall on areas of greater than zero failure probability. Further work throughout the watershed would be necessary to find other failure regions and compare those to predicted values. However with the much reduced spatial extent of the predicted failure regions it would be more feasible to focus efforts of mitigation, as well as to improve model input and assumptions based on areas of erosion potential.

Assumption and input improvements

The assumptions for the fire disturbance module are currently hard coded and do not allow for adjustment to match a different region without manually changing the code. The fire disturbance module was developed for use in the Cascades therefore assumptions typically follow that of work done in that region. One instance is the removal of dead trees following fire. While this is a common practice both in the Cascades and Western Montana, it would be beneficial to choose regions where vegetation was removed in order to more accurately represent vegetative surcharge. Currently recovery periods for overstory vegetation are set to 25 years (Laniniand and Lettenmaier 2005). Regional adjustments may be necessary for this value. There is only support for three fire severity classes, where classes for enhanced re-growth or other classes may be added. The uniform application of hydrophobicity has show to over-estimate peak flows following fire. As more becomes understood about the spatial variability of hydrophobicity it would be beneficial to make such changes to the logic of the fire module portion of DHSVM. With the fire disturbance model just recently being finished, revision may see many of these parameters end up as values in the disturbance input file. This would allow for parameters to be adjusted to better match that of the region being modeled.

Model Applications

The three scenarios modeled in this thesis were designed to create results that could be used in a rapid post fire analysis. Currently the amount of time required to create the input layers and files would most likely exceed the time necessary to get results to those doing post-fire planning. If the results of a DHSVM analysis on fire were deemed valuable to post-fire planning, then much of the data would need to be prepared prior to a fire. Layers such as vegetation, soils, and DEM would need to be prepared by region or state. Predefined classes for soils and vegetation would require the appropriate parameters in the input files. With the majority of the data input files ready, the remaining input would be the fire severity layer. Preparing weather data can be quite lengthy depending on available data sources. Formats such as Parameter-elevation Regressions on Independent Slopes Model (PRISM) might be a potential solution to avoid intensive data formatting as DHSVM accepts the PRISM data format. By applying similar techniques to those used on the Copper Creek watershed, combined with measurements of streamflow and mass wasting events following fire, a thorough understanding of the performance of the model could be understood. With many inputs available, DHSVM could potentially be adapted as a valuable tool in post-fire assessment.

Longer term applications involving DHSVM and fire can certainly be looked at due to the per pixel modeling framework by which DHSVM runs. The resolution of the output allows for changes to be seen over time. Potential applications could look at changes in geomorphology due to erosion following post fire events or recovery of vegetation following fire and its affects on hydrologic response. Applications such as these will test DHSVM and its ability to model processes that occur within the landscape and help to better understand the complex interactions fire has with the ecosystem.

Bibliography

Bassette, G. 2005. personal communication.

Brown, J.K., Smith, J.K. eds. 2000. Wildland fire in ecosystems: effects of fire on flora. Gen. Tech. Rep. RMRS-GTR-42-vol.2. Ogden, UT: U.S. Department of Agriculture, Forest Service, Rocky Mountain Research Station. 257.

Doten, C.O., L.C. Bowling, E.P. Maurer, J.S. Lanini, and D.P. Lettenmaier: 2006. A spatially distributed model for the dynamic prediction of sediment erosion and transport in mountainous forested watersheds, Water Resources Research 42: W04117.

DeBano, L., D. Neary, and P. Ffolliott. 1998. Fire's Effects on Ecosystems John Wiley and Sons. 333 p.

Dyrness, C.T. 1976. Effects of wildfire on soil wettability in the high Cascades of Oregon. USDA Forest Service Research Paper PNW-202. Portland, OR.

Farley, S. 2003. personal communication.

Hammond, C., D. hall, S. Miller and P. Swetik, 1992. Level I Stability Analysis (LISA) Documentation for version 2.0. USDA Intermountain Research Station, General Technical Report INT-285.

Huffman, E.L., L.H. MacDonald, and J.D. Stednick. 2001. Strength and persistence of fire-induced soil hydrophobicity under ponderosa and lodgepole pine, Colorado Front Range. Hydrological Processes 15:2877–2892.

Kamps, A. 2005. personal communication.

Key, C.H., and N.C. Benson. 2003. The Normalized Burn Ratio (NBR): A LANDSAT TM Radiometric Measure of Burn Severity. Date Accessed: 15 Aug. 2006 [Online] http://www.nrmsc.usgs.gov/research/ndbr.htm.

Lanini J.S., and D.P. Lettenmaier, 2006. Effects of Climate and Fire Regime on Post-fire Sediment Delivery in Pacific Northwest Forests, Geophysical Research (submitted).

Lanini, J.S., and D.P. Lettenmaier. 2005. Fire model documentation. Department of Civil and Environmental Engineering, University of Washington, Seattle. 26 p.

Lanini, J.S. 2004. Oral Presentation. DHSVM Users Group Meeting, Oral Presentation. Hydrology Research Group, University of Washington. Date Accessed: 15 Oct. 2006 [Online] http://www.hydro.washington.edu/Lettenmaier/Presentations/2004/lanini_dhsvm_users_mar_2004.ppt.

Lettenmaier, D.P. 2006. Land Surface Hydrology Research Group, University of Washington. Date Accessed: 15 Aug. 2006 [Online] http://www.hydro.washington.edu/Lettenmaier/Models/DHSVM/index.shtml.

Moody, J.A., and D.A. Martin. 2001. Initial Hydrologic and Geomorphic Response Following a Wildfire in the Colorado Front Range. Earth Surface Processes and Landforms 26:1049-1070.

Mulkey, L. 1980. An Approach To Water Resources Evaluation of Non-Point Silvicultural Sources (A Procedural Handbook). Forest Service, United States Department of Agriculture; Environmental Research Laboratory Office of Research and Development U.S. Environmental Protection Agency Athens, Georgia, Washington, D.C.

Nash, J.E., and J.V. Sutcliffe. 1970. River flow forecasting through conceptual models part 1 - A discussion of principles. Journal of Hydrology 10:282-290.

Nave, C.R. 2005. HyperPhysics, Georgia State Univeristy. Date Accessed: 15 Aug. 2006 [Online] http://hyperphysics.phy-astr.gsu.edu/hbase/kinetic/relhum.html.

Neitsch, S.L., J.G. Arnold, J.R. Kiniry, J.R. Williams, and K.W. King. 2002. Soil and Water Assesment Tool Theoretical Documentation, Version 2000. Grassland, Soil and Water Research Laboratory Blackland Research and Extention Center, Temple Texas.

Neary, D.G. and P.F. Ffolliott. 2005a. Part B: The water resource: Its importance characteristics, and general response to fire. IN: Wildland fire in ecosystems: effects of fire on soils and water. Gen. Tech. Rep. RMRS-GTR-42-vol.4. Ogden, UR. USDA Forest Service, Rocky Mountain Station. Pp.95-106.

Neary, D.G., P.F. Ffolliott and J.D. Landsberg. 2005b. Chaper 5: Fire and Streamflow Regimes. IN: Wildland fire in ecosystems: effects of fire on soils and water. Gen. Tech. Rep. RMRS-GTR-42-vol.4. Ogden, UR. USDA Forest Service, Rocky Mountain Station. Pp.107-118.

Neary, D.G., K.C. Ryan, L.F. DeBano, Eds. 2005c. Wildland fire in ecosystems: effects of fire on soils and water. Gen. Tech. Rep. RMRS-GTR-42-vol.4. Ogden, UT. USDA Forest Service, Rocky Mountain Station. 250 p.

Nickless, R., E. Boldt and C. Neesvig. 2002. Rainfall events and their effect on severly burned areas of western Montana following the forest fires of 2000. National Weather Service. Western Regional Technical Attachment No. 02-12 Accessed 21 March, 2006 at http://www.wrh.hoaa.gov/wrh/02TAs/0212/index.html.

Nickless, R. 2006. personal communication.

Redmond, R.L. 1996. Mapping existing vegetation and land cover across western Montana and northern Idaho. Wildlife Spatial Analysis Lab Montana Cooperative Wildlife Research Unit, The University of Montana, Missoula, MT. Accessed 15 March 2006 at http://www.wru.umt.edu/reports/silc/.

Robichaud, P.R. 2000. Fire effects on infiltration rates after prescribed fire in northern Rocky Mountain forests, USA. Journal of Hydrology 231-232:220-229.

Robichaud, P.R. 2005. Measurement of post-fire hillslope erosion to evaluate and model rehabilitation treatment effectiveness and recovery. International Journal of Wildland Fire 14:475-485.

Robichaud, P.R., and R.E. Brown. 2002. Silt Fences: An Economical Technique for Measuring Hillslope Soil Erosion. General Technical Report RMR -GTR-94. USDA - Forest Service.

Singh V.P. 1995. Chapter 1: Watershed Modeling. IN: Models of Watershed Hydrology. Dept. of Civil and Environment Engineering, Louisiana State University. pp 1-22.
Spokas, K., and F. Forcella. 2006. Estimating hourly incoming solar radiation from limited meteorological data. Weed Science 54:182-189.

Storck, P., L. Bowling, P. Wetherbee, and D. Lettenmaier. 1998. Application of a GIS-based distributed hydrology model for prediction of forest harvest effects on peak stream flow in the Pacific Northwest. Hydrological Processes 12:889 - 904.

Stuart, B., S. Farley, J. Kendley, S. Scott, L. Olsen, L. Burns, P. Shanley, B. Badgett, M. Scott, C. Fisher, L. Walch, A. Harper, J. Kaiser, M. Geary, E. Lundberg, C. McKenna, D. Huffner, and C. Davis. 2003. Snow-Talon Fire Burned Area Emergency (BAER) Report. U.S. Forest Service - Helena National Forest, Lincoln Ranger District. 80 p.

Swanston, D., F. Swanson, and Rosgen. 1980. An approach to water resources evaluation of non-point silvicultural sources. EPA-600/80-80-012. USDA Forest Service and U.S. EPA. 49p.

Thyer, M., J. Beckers, D. Spittlehouse, Y. Alila, and R. Winkler. 2004. Diagnosing a distributed hydrologic model for two high-elevation forested catchments based on detailed stand- and basin-scale data. Water Resources Research 40. (in review)

U.S. Department of Commerce. N.O.A.A., National Weather Service, Office of Hydrology. 1973. Isopluvials of 100-YR 6-HR Precipitation.

Ward, J.L. 2005. personal communication.

Whitaker, A., Y. Alila, J. Beckers, and D. Toews. 2003. Application of the Distrbuted Hydrology Soil Vegetaion Model to Redfish Creek, British Columbia: model evaluation using internal catchment data. Hydrological Processes 17:199-224.

Wicks, J.M. and J.C. Bathurst. 1996. SHESED: a physically based, distributed erosion and sediment yeild component for the SHE hydrological modeling system. Journal of Hydrology. 175. 213-238.

Wigmosta, M.S., B. Nijssen, P. Storck, and D.P. Lettenmaier, 2002: The Distributed Hydrology Soil Vegetation Model, In Mathematical Models of Small Watershed Hydrology and Applications, V.P. Singh, D.K. Frevert, eds., Water Resource Publications, Littleton, CO., p. 7-42.

Wondzell, S.M., and J.G. King. 2003. Postfire erosional processes in the Pacific Northwest and Rocky Mountains regions. Forest Ecology and Management 178:75-87.